

ACTA DE EVALUACIÓN DE LA TESIS DOCTORAL
(FOR EVALUATION OF THE ACT DOCTORAL THESIS)

Año académico (*academic year*): 2017/18

DOCTORANDO (*candidate PHD*): **GOVETTO, ANDREA**
D.N.I./PASAPORTE (*Id.Passport*): ******48591**
PROGRAMA DE DOCTORADO (*Academic Committee of the Programme*): **D420-CIENCIAS DE LA SALUD**
DPTO. COORDINADOR DEL PROGRAMA (*Department*): **BIOLOGÍA DE SISTEMAS**
TITULACIÓN DE DOCTOR EN (*Phd title*): **DOCTOR/A POR LA UNIVERSIDAD DE ALCALÁ**

En el día de hoy 04/05/18, reunido el tribunal de evaluación, constituido por los miembros que suscriben el presente Acta, el aspirante defendió su Tesis Doctoral **con Mención Internacional** (*In today assessment met the court, consisting of the members who signed this Act, the candidate defended his doctoral thesis with mention as International Doctorate*), elaborada bajo la dirección de (*prepared under the direction of*) MARTA SUÁREZ DE FIGUEROA.

Sobre el siguiente tema (*Title of the doctoral thesis*): **GROSOR COROIDEO EN LA DEGENERACIÓN MACULAR ASOCIADA A LA EDAD: UN ESTUDIO TRASVERSAL**

Finalizada la defensa y discusión de la tesis, el tribunal acordó otorgar la CALIFICACIÓN GLOBAL¹ de **(no apto, aprobado, notable y sobresaliente)** (*After the defense and defense of the thesis, the court agreed to grant the GLOBAL RATING (fail, pass, good and excellent)*): SOBRESALIENTE

Alcalá de Henares, a 4 de MAYO de 2017



Fdo. (Signed):

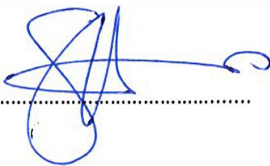


Fdo. (Signed):



Fdo. (Signed):

FIRMA DEL ALUMNO (*candidate's signature*),



Fdo. (Signed):

Con fecha 4 de mayo de 2018, la Comisión Delegada de la Comisión de Estudios Oficiales de Posgrado, a la vista de los votos emitidos de manera anónima por el tribunal que ha juzgado la tesis, resuelve:

- Conceder la Mención de "Cum Laude"
 No conceder la Mención de "Cum Laude"

La Secretaria de la Comisión Delegada



¹ La calificación podrá ser "no apto" "aprobado" "notable" y "sobresaliente". El tribunal podrá otorgar la mención de "cum laude" si la calificación global es de sobresaliente y se emite en tal sentido el voto secreto positivo por unanimidad. (*The grade may be "fail" "pass" "good" or "excellent". The panel may confer the distinction of "cum laude" if the overall grade is "Excellent" and has been awarded unanimously as such after secret voting.*)



Universidad
de Alcalá

COMISIÓN DE ESTUDIOS OFICIALES
DE POSGRADO Y DOCTORADO

En aplicación del art. 14.7 del RD. 99/2011 y el art. 14 del Reglamento de Elaboración, Autorización y Defensa de la Tesis Doctoral, la Comisión Delegada de la Comisión de Estudios Oficiales de Posgrado y Doctorado, en sesión pública de fecha 11 de junio, procedió al escrutinio de los votos emitidos por los miembros del tribunal de la tesis defendida por GOVETTO, ANDREA, el día 4 de mayo de 2018, titulada *GROSOR COROIDEO EN LA DEGENERACIÓN MACULAR ASOCIADA A LA EDAD: UN ESTUDIO TRASVERSAL*, para determinar, si a la misma, se le concede la mención "cum laude", arrojando como resultado el voto favorable de todos los miembros del tribunal.

Por lo tanto, la Comisión de Estudios Oficiales de Posgrado **resuelve otorgar** a dicha tesis la

MENCIÓN "CUM LAUDE"

Alcalá de Henares, 12 de junio de 2018

EL VICERRECTOR DE INVESTIGACIÓN Y TRANSFERENCIA



F. Javier de la Mata

F. Javier de la Mata de la Mata

Copia por e-mail a:

Doctorando: GOVETTO, ANDREA

Secretario del Tribunal: FRANCISCO MUÑOZ NEGRETE

Director/a de Tesis: MARTA SUÁREZ DE FIGUEROA



Universidad
de Alcalá

ESCUELA DE DOCTORADO
Servicio de Estudios Oficiales de
Posgrado

DILIGENCIA DE DEPÓSITO DE TESIS.

Comprobado que el expediente académico de D./D^a ANDREA GOVETTO
reúne los requisitos exigidos para la presentación de la Tesis, de acuerdo a la normativa vigente, y habiendo
presentado la misma en formato: soporte electrónico impreso en papel, para el depósito de la
misma, en el Servicio de Estudios Oficiales de Posgrado, con el nº de páginas: 86 se procede, con
fecha de hoy a registrar el depósito de la tesis.

Alcalá de Henares a 15 de diciembre de 2017



PURIFICACIÓN REVIEJO

Fdo. El Funcionario



Programa de Doctorado en Ciencias de la Salud.

**CHOROIDAL THICKNESS IN NON-NEOVASCULAR VERSUS
NEOVASCULAR AGE-RELATED MACULAR DEGENERATION: A
FELLOW EYE COMPARATIVE STUDY.**

**GROSOR COROIDEO EN LA DEGENERACION MACULAR ASOCIADA
A LA EDAD: UN ESTUDIO TRASVERSAL.**

Tesis doctoral presentada por

ANDREA GOVETTO

Año 2017



Programa de Doctorado en Ciencias de la Salud.

**CHOROIDAL THICKNESS IN NON-NEOVASCULAR VERSUS
NEOVASCULAR AGE-RELATED MACULAR DEGENERATION: A
FELLOW EYE COMPARATIVE STUDY.**

**GROSOR COROIDEO EN LA DEGENERACION MACULAR ASOCIADA
A LA EDAD: UN ESTUDIO TRASVERSAL.**

Tesis doctoral presentada por

ANDREA GOVETTO

Directora:

DRA. MARTA SUAREZ DE FIGUEROA

Alcalá de Henares, 2017

Dña. Marta Suarez de Figueora, Profesora Asociada de Oftalmología de Departamento de Cirugía, Ciencias Médicas y Sociales de la Universidad de Alcalá , como directora y tutora de la presente Tesis Doctoral

CERTIFICA

Que el trabajo titulado " CHOROIDAL THICKNESS IN NON-NEOVASCULAR VERSUS NEOVASCULAR AGE-RELATED MACULAR DEGENERATION: A FELLOW EYE COMPARATIVE STUDY " (GROSOR COROIDEO EN LA DEGENERACION MACULAR ASOCIADA A LA EDAD: UN ESTUDIO TRASVERSAL) ha sido realizada bajo mi dirección por Don ANDREA GOVETTO en e Departamento de Cirugía, Ciencias Médicas y Sociales de la Universidad de Alcalá en colaboracion con la Universidad de California en Los Angeles UCLA (EEUU) y la Universidad Vita-Salute San Raffaele de Milan (ITALIA), y que dicho trabajo reúne los requisitos científicos de originalidad y rigor metodológico suficientes para ser presentado como Tesis Doctoral ante el tribunal que corresponda.

Y para que así conste, se e.1tpide el presente certificado ea Alcalá de llenares, a 23 de Julio de 2017

Marta Suarez de Figueroa





Dr. D. Pedro de la Villa Polo, Coordinador de la Comisión Académica del Programa de Doctorado en Ciencias de la Salud.

INFORMA que la Tesis Doctoral titulada **CHOROIDAL THICKNESS IN NON-NEOVASCULAR VERSUS NEOVASCULAR AGE-RELATED MACULAR DEGENERATION: A FELLOW EYE COMPARATIVE STUDY (GROSOR COROIDEO EN LA DEGENERACIÓN MACULAR ASOCIADA A LA EDAD: UN ESTUDIO TRANSVERSAL)** presentada por D. **ANDREA GOVETTO**, bajo la dirección de la Dra. Dña. Marta Suárez de Figueroa, reúne los requisitos científicos de originalidad y rigor metodológicos para ser defendida ante un tribunal. Esta Comisión ha tenido también en cuenta la evaluación positiva anual del doctorando, habiendo obtenido las correspondientes competencias establecidas en el Programa.

Para que así conste y surta los efectos oportunos, se firma el presente informe en Alcalá de Henares a 08 de noviembre de 2017.



Fdo.: Pedro de la Villa Polo

FINANCIAL DISCLOSURE

There are no financial disclosures to disclose.

ACKNOWLEDGMENTS

This work would not have been possible without the advice and support of many people.

First, and foremost, I would like to thank my tutor Dra Marta Suarez de Figueroa for providing me the opportunity, guidance and mentorship throughout this project.

Special thanks to Dr. David Sarraf and Dr. Hubschman for their patience and guidance during my fellowship at UCLA, and to Prof. Francesco Bandello from Milan who first introduced me to the field of ophthalmology and retina subspecialty.

RESUMEN EN CASTELLANO

OBJETIVOS:

Investigar posibles diferencias de grosor coroideo entre ojos con degeneración macular asociada a la edad (DMAE) no neovascular (NNV) y neovascular (NV).

CENTROS PARTICIPANTES:

Hospital universitario Ramon y Cajal (Madrid, España), Hospital universitario San Raffaele (Milán, Italia) e Instituto Oftalmológico Stein (Los Angeles, Estados Unidos).

METODOS:

Se diseñó un estudio retrospectivo y observacional incluyendo todos los pacientes diagnosticados con DMAE NNV en un ojo y DMAE NV en el ojo contralateral entre enero 2014 y enero 2015 en los centros participantes. Los Ojos con DMAE NNV fueron divididos en subgrupos según los criterios del grupo Beckman: Cambios normales asociados a la edad (grupo 1), DMAE inicial (grupo 2), DMAE intermedia (grupo 3) y DMAE avanzada (grupo 4). El grosor coroideo y retiniano fue medido manualmente usando tomografía de coherencia óptica de dominio espectral (SD-OCT) en modalidad enhanced depth imaging (EDI) desde 1500 μm nasal hasta 1500 μm temporal a la fovea. Pruebas estadísticas paramétricas y no paramétricas fueron empleadas para comparar variables cuantitativas, mientras el test χ^2 fue empleado en las comparaciones entre variables categóricas. Regresiones logísticas fueron empleadas para evaluar la relación entre el grosor coroideo y otras variables de interés.

RESULTADOS:

En este estudio se incluyeron 322 ojos de 161 pacientes de los cuales 102 (63.35%) eran mujeres y 59 (36.65%) eran varones. La edad media era 80.80 ± 8.45 años (rango 58-99 años). El tiempo de seguimiento medio fue de 11.2 ± 10.8 meses (rango 1-38 meses). En ojos con DMAE NNV, la coroides era más gruesa en la zona subfoveal y temporalmente temporal a la fovea, con diferencias estadísticamente significativas si comparadas se comparan con el ojo contralateral con DMAE NV. Las diferencias de grosor coroideo entre DMAE NNV y DMAE NV fueron más marcadas a en estadios más precoces de DMAE NNV.

CONCLUSIONES:

La coroides subfoveal y temporal era fue significativamente más gruesa en DMAE NNV comparada con la DMAE NV de los ojos contralaterales. El adelgazamiento coroideo fue más significativo en estadios avanzados de la DMAE NNV.

ABSTRACT

PURPOSE:

To investigate the possible differences in choroidal thickness (CT) between non-neovascular (NNV) and neovascular (NV) age-related macular degeneration (AMD).

METHODS:

A retrospective, observational chart review of consecutive patients diagnosed with NNV AMD in one eye and with NV AMD in the fellow eye was carried out. NNV AMD was classified into four subgroups according to the Beckman Initiative for Macular Research AMD Classification Committee Meeting. CT was manually assessed using enhanced depth imaging optical coherence tomography from 1500 mm nasal to 1500 mm temporal to the fovea. Parametric and nonparametric tests were used to compare quantitative variables, a χ^2 test was used to compare categorical variables and logistic regression was used to evaluate associations of CT with other variables of interest.

RESULTS:

In this study, 322 eyes from 161 patients were included and 102 (63.35%) were female and 59 (36.65%) were male, with a mean age of 80.80 ± 8.45 years (range 58–99 years). Mean follow-up was 11.2 ± 10.8 months (range 1–38 months). In NNV AMD eyes, the choroid was significantly thicker in the subfoveal and temporal regions of the macula, if compared with NV AMD fellow eyes. Differences in CT between NNV AMD and NV AMD fellow eyes were higher at earlier stages of NNV AMD.

CONCLUSIONS:

Subfoveal and temporal choroid was significantly thicker in NNV AMD compared with NV AMD fellow eyes. There was a significant choroidal thinning at advanced stages of NNV AMD.

CONTENTS

- I.INDEX**
- II.LIST OF ABBREVIATIONS**
- III.LIST OF FIGURES**
- IV.LIST OF TABLES**

I. INDEX

1	INTRODUCTION	8
1.1	NORMAL CHOROIDAL ANATOMY AND PHYSIOLOGY	9
1.1.0	Physiology of the Choroid.....	9
1.1.1	Normal Vascular Anatomy of the Choroid.....	11
1.2	AGE RELATED MACULAR DEGENERATION	13
1.2.0	Epidemiology	13
1.2.1	Clinical classification.....	16
1.2.1	Non-neovascular form	20
1.2.2	Neovascular form	23
1.3	ROLE OF THE CHOROID IN THE PATHOGENESIS OF AGE RELATED MACULAR DEGENERATION.....	26
1.3.1	Vascular model of Age Related Macular Degeneration	26
1.3.2	The aging choroid.....	27
1.4	IMAGING THE CHOROID.....	30
1.4.1	Fluorescein angiography.	30
1.4.2	Indocyanine green angiography.	31
1.4.3	Ultrasonography	33
1.4.4	Spectral-Domain Optical Coherence Tomography	34
1.5	IMAGING THE CHOROID WITH SD-OCT	35
1.5.1	Enhanced Depth Imaging	35
1.5.2	Choroidal thickness measurements using EDI SD-OCT imaging	37
1.5.3	Reproducibility of choroidal thickness.....	39
1.5.4	Normal choroidal thickness and its variations.....	39
1.5.5	Qualitative analysis of the choroid with EDI SD-OCT analysis	41
2	MATERIAL AND METHODS.....	43
2.1	Study design, participating centers, study population	44
2.2	Exclusion criteria	44

2.3	Imaging acquisition	44
2.4	Choroidal thickness assessment.....	51
2.5	Statistical analysis.....	53
3	RESULTS.....	54
3.1	Included study population	54
3.2	Best Corrected Visual Acuity.....	54
3.3	Anti-Vascular-Endothelial Growth Factor Injections	55
3.4	Associations of choroidal thickness with age	55
3.5	Choroidal thickness in the study population	56
4	DISCUSSION	62
5	CONCLUSIONS	71
6	REFERENCES	72

II. LIST OF ABBREVIATIONS

EDI: enhanced depth imaging

SD-OCT: spectral-domain optical coherence tomography

CT: choroidal thickness

NV: neovascular

NNV: non-neovascular

AMD: age-related macular degeneration

NIE: national eye institute

AREDS: age-related eye disease study

GA: Geographic atrophy

CNV: choroidal neovascularization

PED: pigment epithelium detachment

RPE: retinal pigment epithelium

VEGF: vascular-endothelial growth factor

ICG: Indocyanine green

BCVA: best-corrected visual acuity

logMAR: logarithm of the minimum angle of resolution

RT: retinal thickness

OCT-A: optical coherence tomography angiography

III. LIST OF FIGURES

Figure 1: Photomicrograph of the choroid in the macular area of a 65 years old male.

Figure 2: Projections of AMD cases divided by race. Data from the united states national eye institute.

Figure 3: AMD projections for years 2020, 2030 and 2040.

Figure 4: Multicolor pictures: normal eyes and normal ageing changes.

Figure 5: Multicolor pictures: early and intermediate AMD

Figure 6: Multicolor pictures: late non-neovascular and neovascular AMD

Figure 7: Photomicrograph of drusen.

Figure 8: Multimodal imaging of reticular pseudodrusen in a 70 years old male.

Figure 9: Multimodal imaging of bilateral geographic atrophy in a 90 years old female.

Figure 10: Multimodal imaging of a disciform scar.

Figure 11: Multimodal imaging of RPE rip.

Figure 12: Photomicrograph pictures of the choroid, same magnification.

Figure 13: Comparison of fluorescein and indocyanine green angiography in the same eye.

Figure 14: B-Scan

Figure 15: SD-OCT cross-sectional scan of a normal macula.

Figure 16: Normal SD-OCT settings.

Figure 17: SD-OCT with and without EDI module.

Figure 18: Manual measurement of choroidal thickness.

Figure 19: Automatic segmentation of the choroid.

Figure 20: Comparison of histologic and SD-OCT EDI imaging of the choroid.

Figure 21: Choriocapillaris, Sattler's and Haller's layers, and the choroid–scleral junction as seen with EDI OCT .

Figure 22: Multicolor picture, normal ageing changes.

Figure 23: Multicolor picture, early AMD.

Figure 24: Multicolor picture, intermediate AMD.

Figure 25: Multicolor picture, late AMD.

Figure 26: Multimodal imaging of geographic atrophy.

Figure 27: Choroidal and retinal thickness assessment.

Figure 28: Yearly mean decrease in CT in NVAMD and NNVAMD.

Figure 29: Choroidal thickness evaluation.

Figure 30: Comparison of choroidal thickness between NNV AMD group 1 (normal aging changes) and NV AMD.

Figure 31: Comparison of choroidal thickness between NNV AMD group 2 (early AMD) and NV AMD.

Figure 32: Comparison of choroidal thickness between NNV AMD group 3 (intermediate AMD) and NV AMD.

Figure 33: Comparison of choroidal thickness between NNV AMD group 4 (advanced AMD) and NV AMD.

Figure 34: Choroidal thickness in non-neovascular versus neovascular fellow eye: subgroup analysis.

Figure 35: Optical Coherence Tomography Angiography in age related macular degeneration.

IV. LIST OF TABLES

Table 1: Choroidal Thickness in Neovascular (n=161) versus Non-Neovascular (n=161) fellow eyes.

Table 2: Comparison of Choroidal Thickness between the four subgroups of non-neovascular age-related macular degeneration: Groups 1 vs 2 vs 3 vs 4.

Table 3: Correlation between choroidal and retinal thickness in both NV and NNV AMD.

1. INTRODUCTION

The recent introduction of enhanced depth imaging (EDI) spectral-domain optical coherence tomography (OCT) techniques, first described by Margolis and Spaide in 2009,¹ has resulted in more robust investigation of the choroid, including the study of choroidal thickness (CT) and morphology, in a broad spectrum of ocular diseases.²⁻¹¹

While EDI OCT imaging acquisition is simple and straightforward, the analysis and interpretation can be challenging and can vary significantly among individuals, and may be influenced by multiple ocular and extraocular factors that are difficult to control.¹² Such variability may represent a significant limitation when comparing CT in a study population versus a control group.²

The choroid may play a role in the pathogenesis of both neovascular (NV) and non-NV (NNV) age-related macular degeneration (AMD), as reduction in choroidal perfusion and associated outer retinal ischemia has been described in both forms of this disease.¹³⁻¹⁶ Therefore, considering the intimate relationship between the outer retina and the choroid, it would be reasonable to expect a correlation between choroidal status and AMD progression.

While some reports have shown a significant association between CT and AMD status, specifically a thinner choroid at later stages of the disease,^{17,18} other published studies have not confirmed this finding.^{3,19-23} In addition, studies investigating possible differences in CT between NNV AMD and NV AMD have been inconclusive.²³

The variable results in the literature may be explained by the lack of a comparative fellow-eye study, which may significantly reduce the risk of bias due to confounders, and may overcome the issue of CT variability among different individuals. Therefore, we

designed a retrospective, multicenter observational and comparative study to investigate variations of CT between eyes with various grades of NNV AMD and fellow eyes with NV AMD.

In this thesis, we will summarize the anatomy, histology, physiology and pathophysiology of the choroid and the retina in AMD, and discuss the results of our study investigating the anatomical variations of the choroid in the different stages of AMD.

1.1 NORMAL CHOROIDAL ANATOMY AND PHYSIOLOGY

1.1.0 Physiology of the Choroid

The word choroid comes from the ancient Greek: korio-aydez, for korio (corio): a membrane around the fetus, and aydez (ειδης): that looks like. In Latin this word meant network. Approximately 95% of the blood flow in the eye goes to the uvea, with the choroid accounting for more than 70%.²⁴

The choroid has the highest blood flow per unit weight of any tissue in the body, and its main function is to supply oxygen and metabolites to the outer retina, retinal pigment epithelium, and the fovea.²⁵

The fovea centralis is a small, central area of the macula characterized by the highest density of cone photoreceptors. The photoreceptors have an extremely high necessity of oxygen, and are replete with mitochondria. This cells have the highest rate of use of oxygen per unit weight of any other tissue of the body.²⁶

Its characteristic anatomical features include the presence of large membrane-lined lacunae, which can dramatically increase their volume and, therefore, causing the increase of the thickness of the choroid.²⁷

Moreover, the choroid contains nonvascular smooth muscle cells, which contraction may result in choroidal thinning, opposing the thickening caused by expansion of the lacunae.

The thickness of the choroid is extremely variable among individuals, and may be influenced by a broad spectrum of factors such as age, axial length, systemic blood pressure, ocular perfusion pressure, diurnal fluctuations, smoking, anterior chamber depth, lens thickness, corneal curvature, obstructive sleep apnea syndrome, body mass index, use of phosphodiesterase inhibitors, and others.²⁸⁻³⁸

The choroid has also intrinsic innervation, which may control the smooth muscle cell and may modulate choroidal blood flow as well. The intrinsic choroidal neurons receive sympathetic, parasympathetic and nitrergic innervation.

The choroid has several functions: Its vasculature is the major supply for the outer retina, and an impairment of the flow of oxygen from choroid to the retina may cause AMD. The choroidal blood flow, which is as great as in any other organ, may also have thermoregulatory functions.³⁹ The choroid also contains secretory cells, probably involved in the modulation of the blood flow and scleral growth.³⁹

1.1.1 Normal Vascular Anatomy of the Choroid

The Choroid is occupied by vessels divided in three well-defined vascular layers, which can be differentiated based on their location and lumen diameter. The short and long ciliary arteries supply blood to the choroidal vasculature, while 4 to 6 vortex veins remove blood from this system.

The thinner and innermost of these three layers is the *choriocapillaris*, a dense and continuous network of capillaries bordering Bruch's membrane. The capillaries are fenestrated, allowing the passage of molecules through pores measuring 60-70nm (figure 1, A). Such capillaries branch from the medium- and small-sized vessels in the intermediate layer of the choroid: *Sattler's layer* (Figure 1, B).

Finally, *Haller's layer* is the outermost layer and consists of posterior ciliary arteries and larger veins (figure 1, C). The thickness of this layer is maximum at the posterior pole of the eye, in the macular region.

Differently from the retina, the vascular hierarchy in the choroid is lobular, similar to the kidney's lobules. Choroidal circulation is an end-arterial vascular bed with segmental blood flow and watershed zones and this is of great clinical importance, as the reaction of the choroid to different pathological mechanisms, including ischemia, may differ according to the location relative to the watershed zones.⁴⁰ In this regard, the macular region seems to be particularly susceptible to ischemia, as in this area there is a confluence of multiple watershed zones. The poor vascularity of the macular choroid may be relevant in the pathophysiology of diseases like AMD.^{39,40}

Figure 1



Photomicrograph of the choroid in the macular area of a 65 years old male. A: Choriocapillaris; B: Sattler's layer; C: Haller's Layer.

1.2 AGE RELATED MACULAR DEGENERATION

1.2.0 Epidemiology

It is estimated that 8% of the worldwide population has age-related macular degeneration (AMD).⁴¹

AMD is the leading cause of legal blindness in patients aged 65 or over, and it is the most common cause of blindness in the western world. Numerous population-based studies of age-related macular degeneration have been reported worldwide, with results suggesting racial or ethnic differences in disease prevalence.⁴¹

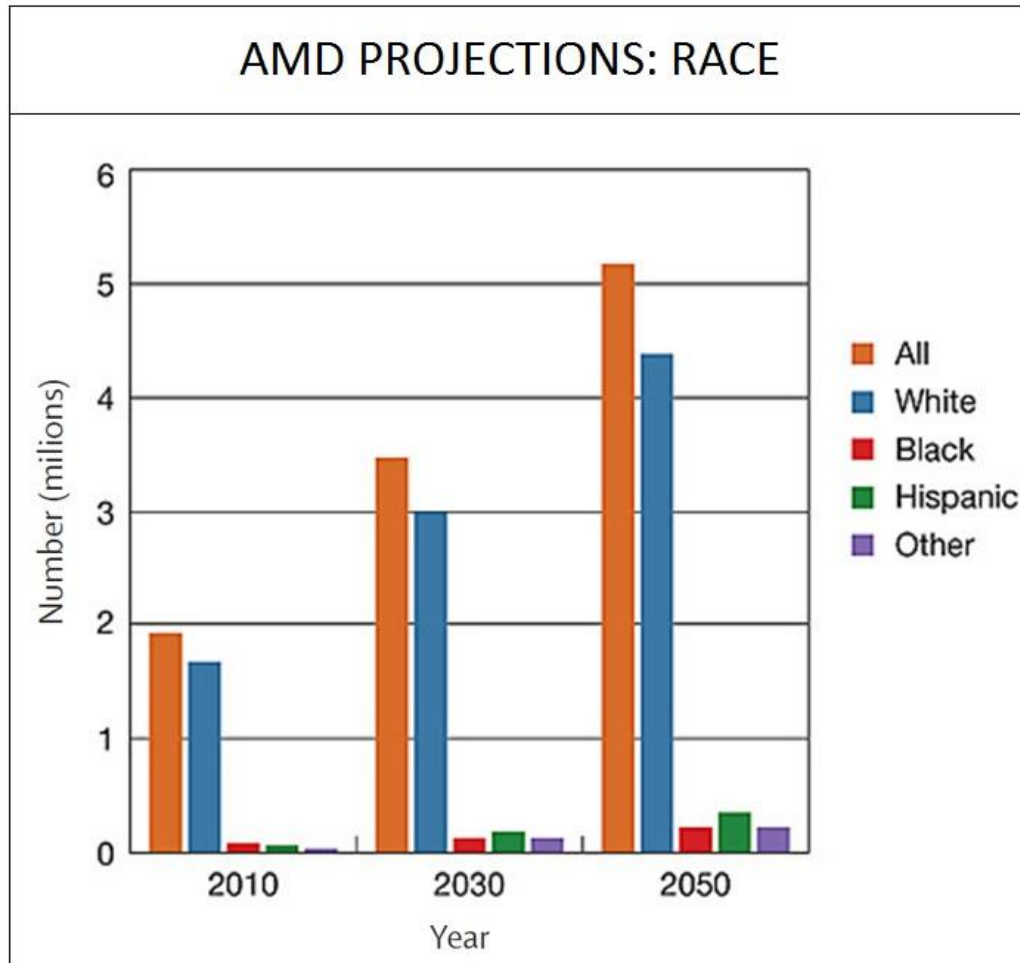
Data from the United States National Eye Institute (NIE) in the year 2010 shows a prevalence rate of 14% for white Americans aged 80 or over, confirming that Caucasians have the greatest likelihood of developing AMD. In 2010, 2.5 percent of white adults age 50 and older had AMD.

By comparison, AMD affected 0.9 percent each of blacks, Hispanics and people of other races (available at <https://nei.nih.gov/eyedata/amd>).

Women generally have a longer life expectancy than men and are therefore more likely to develop age-related eye diseases such as AMD. In 2010, 65 percent of AMD cases were in women compared with 35 percent in men in the United States.

By 2050, the estimated number of people with AMD in the United States is expected to more than double from 2.2 million to 5.4 million. White Americans will continue to account for the majority of cases. However, Hispanics will see the greatest rate of increase, with a nearly six-fold rise in the number of expected cases from 2010 to 2050 (figure 2).

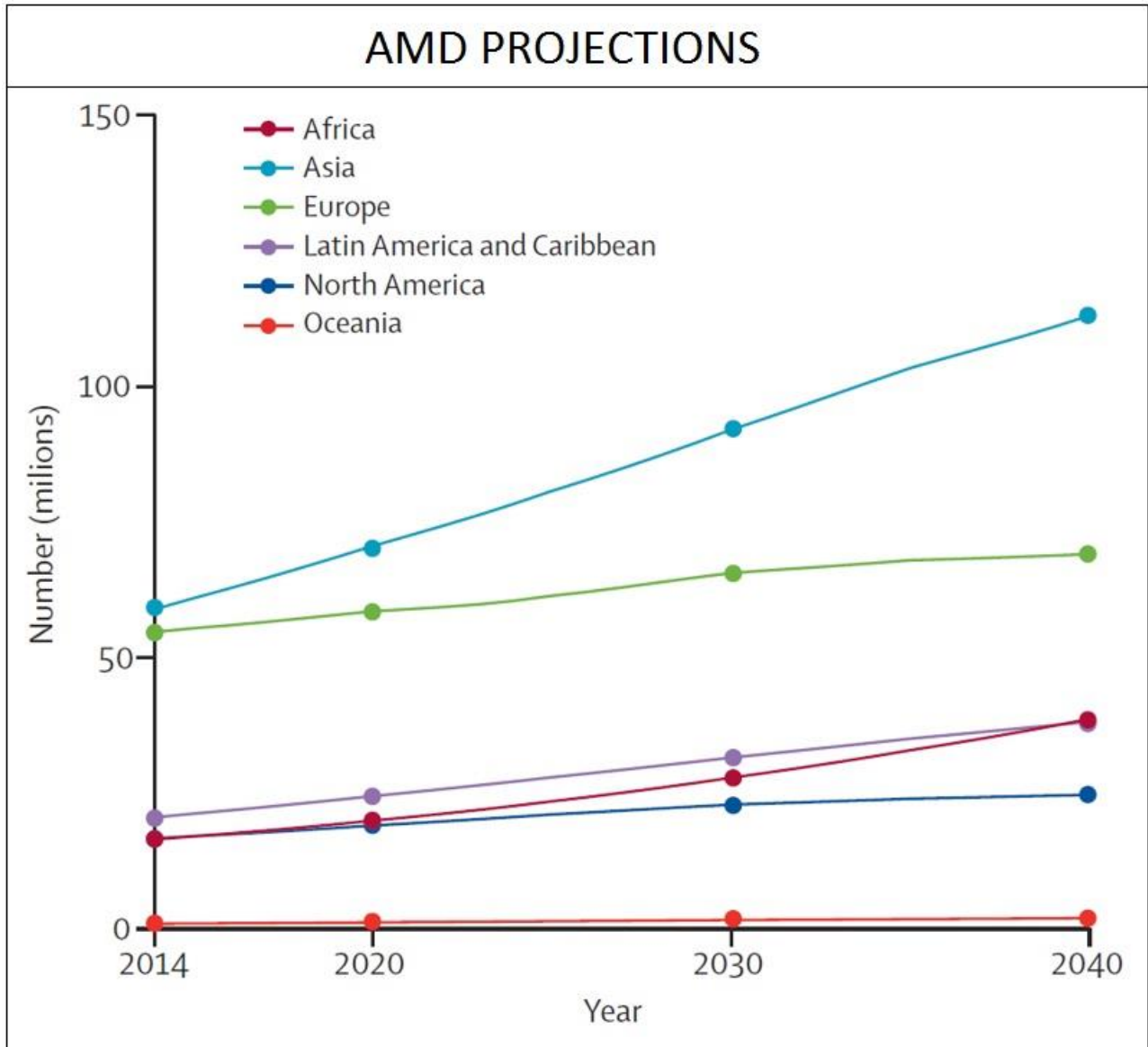
Figure 2



Projections of AMD cases divided by race. Data from the united states national eye institute. Data available at: <https://nei.nih.gov/eyedata/amd>.

By 2020, the global worldwide projected cases of any age-related macular degeneration are 196 million, rising to 288 million in 2040, with the largest number of cases in Asia. In 2040, Europe is expected to be second to Asia in the number of projected cases (69 million), followed by Africa (39 million), Latin America and the Caribbean (39 million), North America (25 million), and Oceania (2 million) as shown in figure 3.⁴¹

Figure 3



AMD projections for years 2020, 2030 and 2040. Asia lead the projection of expected AMD cases followed by Europe.

1.2.1 Clinical classification

Recently, the Beckman Initiative for Macular Research Classification Committee proposed a new clinical classification system for AMD. The new clinical classification is simpler, user-friendly and more suitable to normal clinical practice if compared to the former Age-Related Eye Disease Study (AREDS) staging system.⁴²

Patients with no visible drusen or pigmentary abnormalities are considered as without signs of AMD (figure 4,A) . Patients with small drusen ($<63\mu\text{m}$), or drupelets, are considered to have normal aging changes with no clinically relevant increased risk of late AMD developing (figure 4,B).

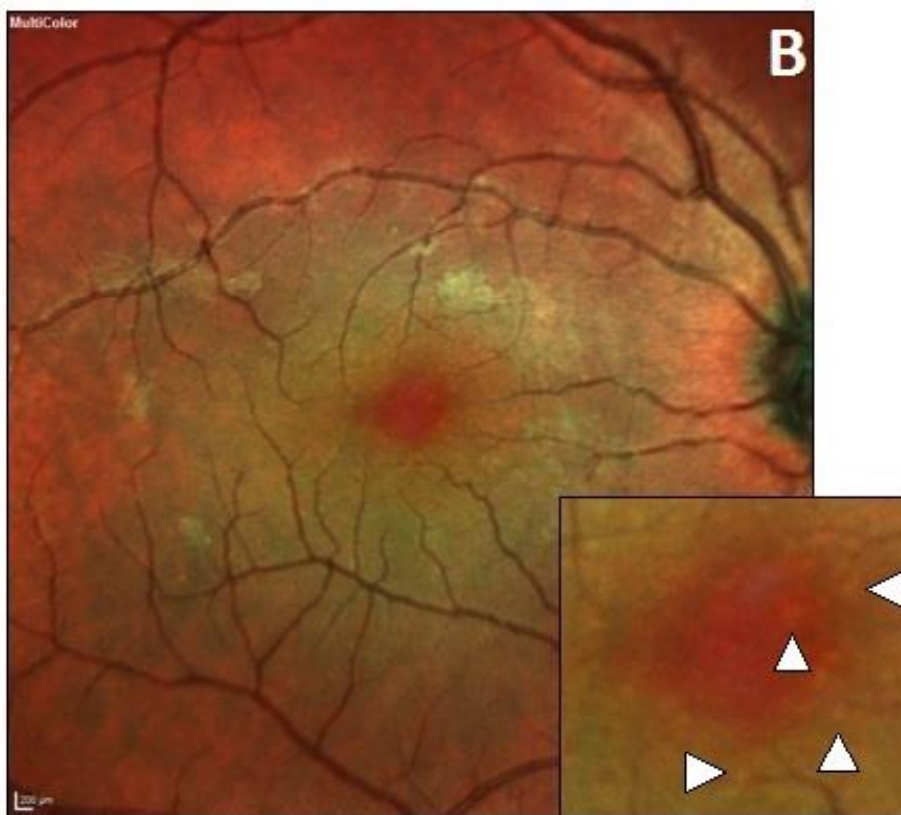
Patients with AMD are divided into three grades:

- **Early AMD:** Patients with medium drusen ($\geq 63 < 125\mu\text{m}$), but without pigmentary abnormalities (figure 5,A).
- **Intermediate AMD:** Patients with large drusen ($\geq 125\mu\text{m}$) or with retinal pigment epithelium (RPE) abnormalities associated with at least medium drusen ($\geq 63 < 125\mu\text{m}$), as seen in figure 5,B.
- **Late AMD:** Patients with lesions associated with neovascular AMD or geographic atrophy (figure 6, A, B).

Figure 4



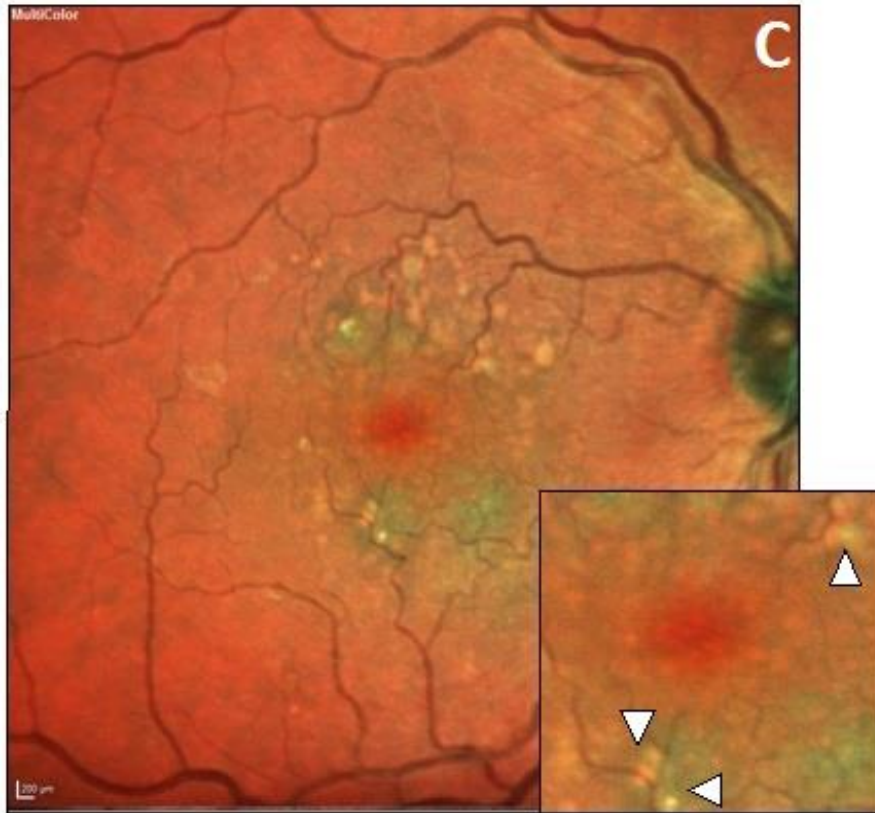
A: Multicolor picture.
Normal eye



B: Multicolor picture.
Normal aging
changes.

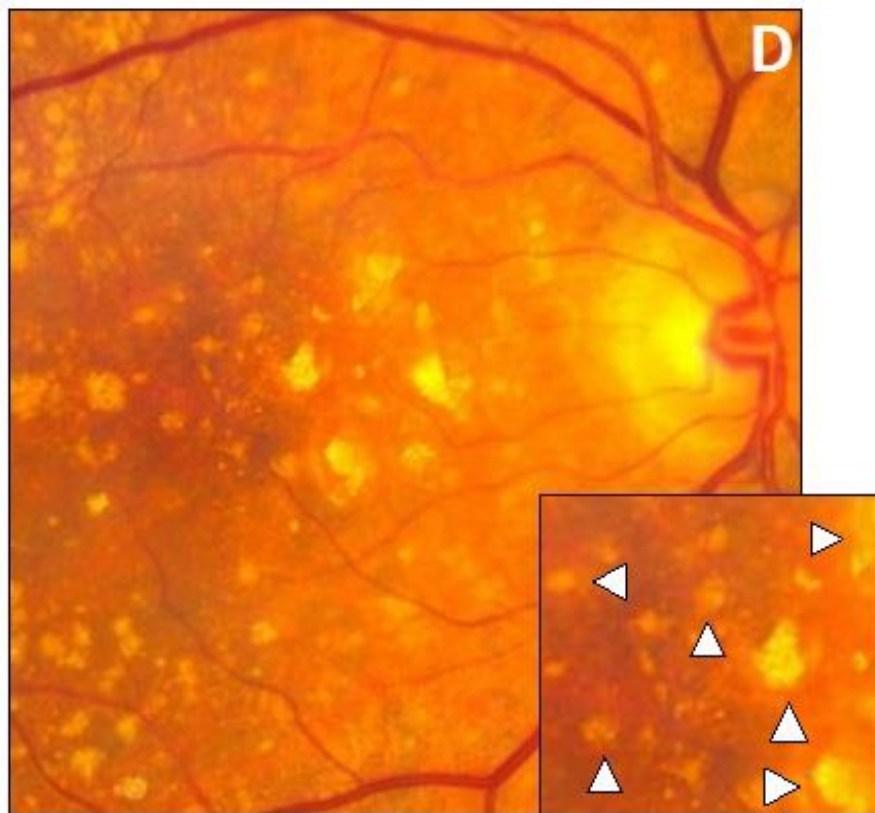
Few droplets can be seen in the foveal region (white arrows).

Figure 5



**C: Multicolor picture.
Early AMD.**

Hard drusen without pigmentary abnormalities can be seen in the foveal region (white arrows).



**D: Multicolor picture.
Intermediate AMD.**

Numerous soft, confluent drusen are visible in the foveal and macular region (white arrows).

Figure 6



E: Multicolor picture.
Late non-neovascular
AMD, geographic
atrophy.

A large area of RPE
atrophy can be seen in
the parafoveal region
(white arrows)



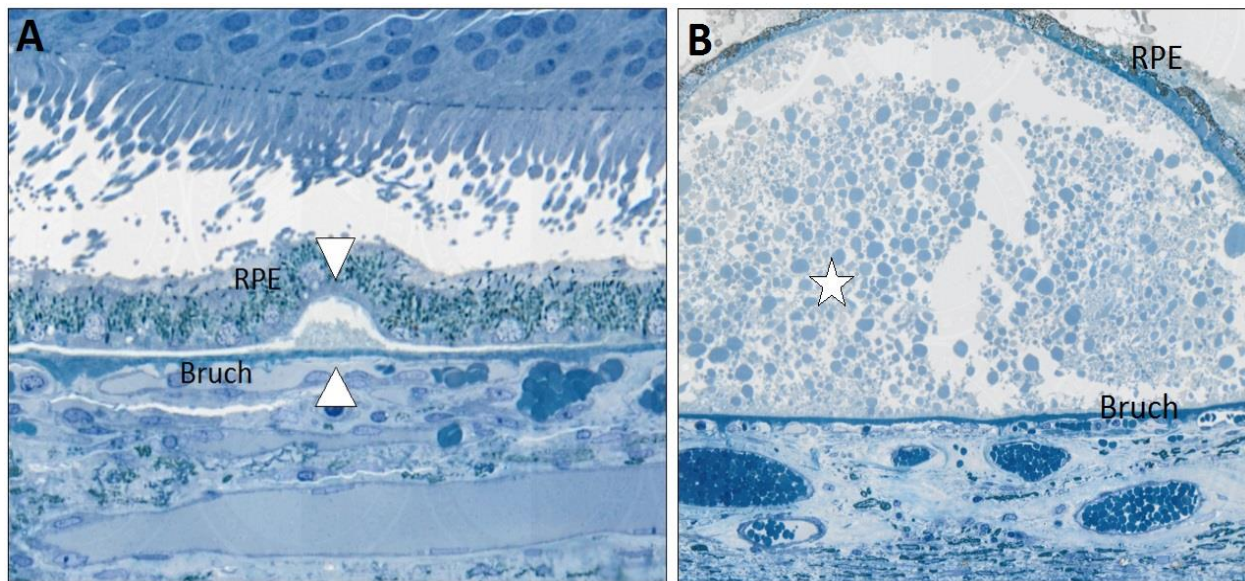
F: Multicolor picture.
Late neovascular
AMD, macular
hemorrhage.

Choroidal
neovascularization and
subretinal hemorrhage
(white arrows)

1.2.3 Non-neovascular form

Non neovascular AMD (NNV-AMD), also commonly called “dry” AMD, is defined as AMD without the presence of choroidal neovascularization. A common sign of NV-AMD is the presence of drusen. Drusen are yellowish deposits of extracellular material which accumulates between Bruch’s membrane and the retinal pigment epithelium, as seen in figure 7. Classically they are divided between *hard* (figure 7,A) and *soft* drusen (figure 7,B). Soft drusen are normally larger than hard drusen, and may aggregate between them.

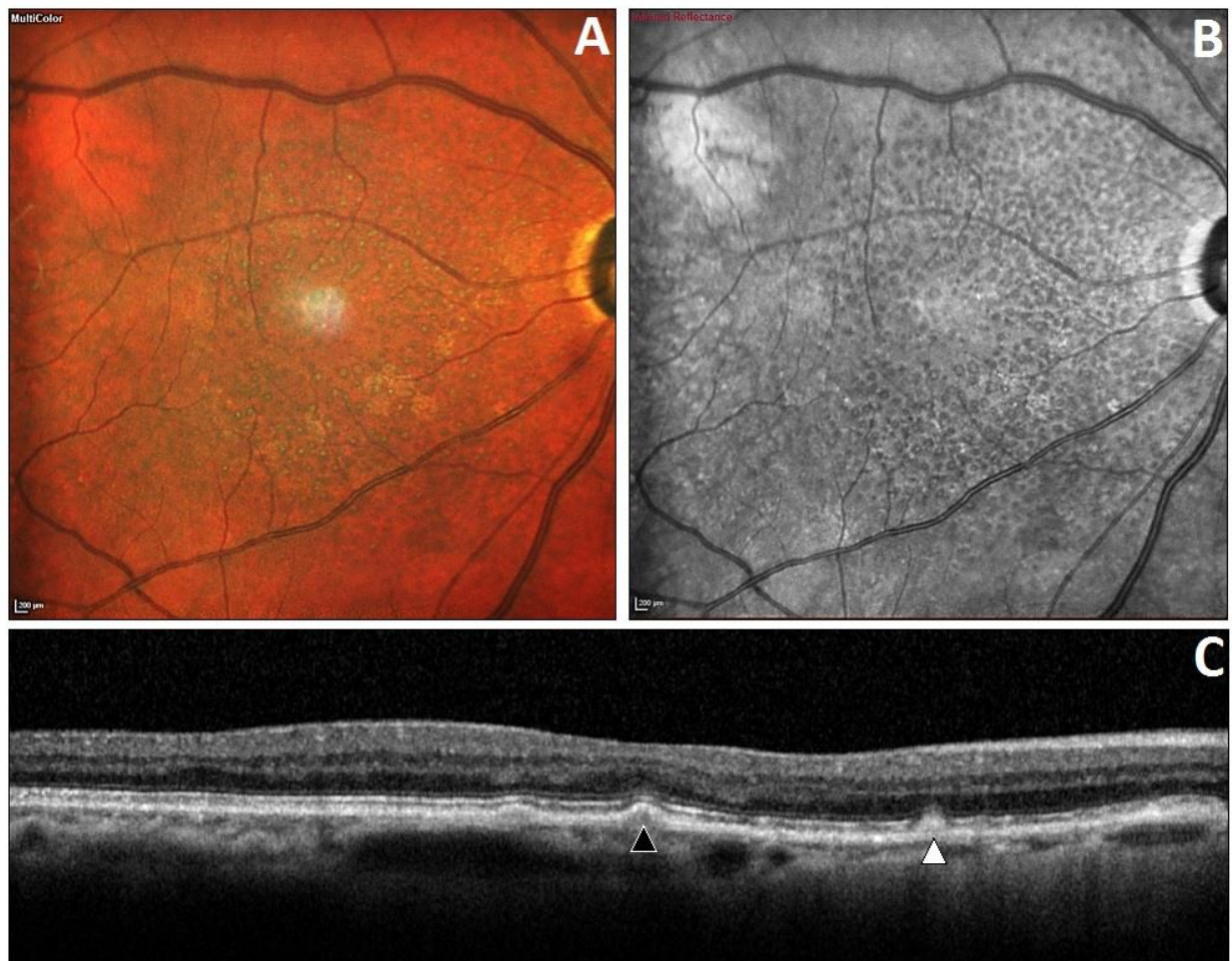
Figure 7



Photomicrograph of drusen. A: Hard drusen. 70 years old woman. The accumulation of extracellular material between the Bruch membrane and the RPE (white arrows) caused a small, focal elevation of the RPE. **B. Soft drusen.** 85 years old male. Diffuse elevation of the RPE due to significant deposition of extracellular material.

Other drusenoid-like lesions known as *reticular pseudodrusen* may resemble the anatomical aspects of classic drusen, but their location is over the retinal pigment epithelium, as seen in figure 8.

Figure 8



Multimodal imaging of reticular pseudodrusen in a 70 years old male. A: Multicolor. Multiple well-defined yellow spots are visible throughout the macular region. **B: infrared reflectance.** The spots are hypo reflective. **C: Optical coherence tomography.** Classic drusen (black arrow) lies beneath the RPE, while reticular pseudodrusen (white arrow) lies over the RPE.

Drusen can also be divided by size. They are considered to be *small* when their diameter is less than 63µm, *medium* when their diameter is more or equal than 63µm and less than 125µm, and *large* when their diameter is more or equal than 125µm.⁴²

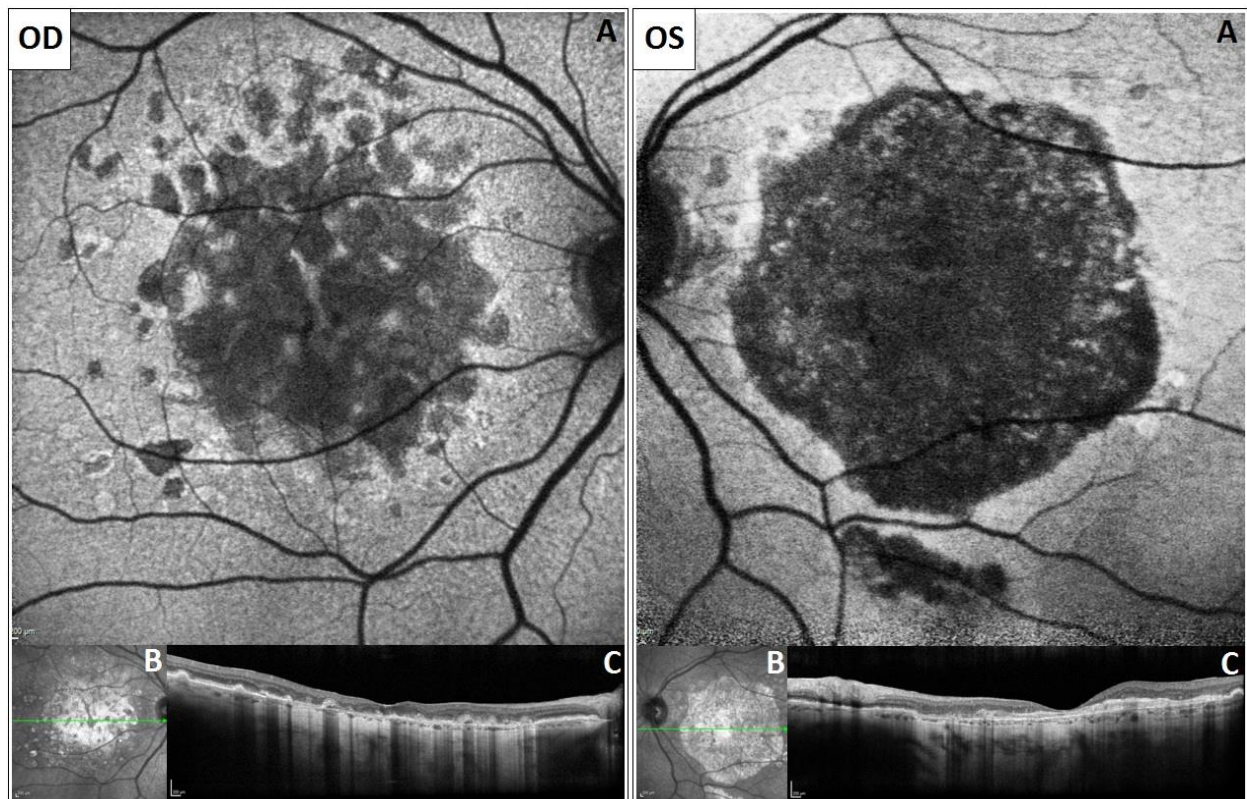
The presence of confluent soft drusen is considered as a risk factor for the progression of AMD. In the AREDS study it was reported that the risk of conversion to the neovascular form of AMD within 5 years is extremely low for early AMD patients (1%). The risk increases in case of patients with unilateral intermediate AMD (6%) and becomes considerable in patients with bilateral intermediate AMD (25%).⁴³

In other prospective studies, 5% of the patients with intermediate AMD evolved to *Geographic atrophy* (GA) within 5 years.⁴⁴

GA is the end stage of the non-neovascular form of AMD as is defined as any clearly delineated round or oval hypopigmentation or depigmentation or absence of the retinal pigment epithelium, in which choroidal vessels are more visible. It is better imaged with autofluorescence (figure 9). Normally, to be considered as GA such area has to be a diameter of at least 150-350µm.⁴²

In earliest NNV-AMD stages (early and intermediate) the visual acuity is normally not compromised [ref], while at late stage, known as *geographic atrophy* the important atrophy of the retinal pigment epithelium and the subsequent photoreceptor loss may significantly decrease the visual acuity of the patient.⁴³

Figure 9



Multimodal imaging of bilateral geographic atrophy in a 90 years old female. A: Autofluorescence. Geographic atrophy is seen as a large, confluent and patchy area of hypoautofluorescence, due to RPE atrophy. **B. Red free image. C. Optical Coherence tomography.** In cross sectional images the RPE in the macular region is atrophic. Note the significant thinning of the retina.

1.2.4 Neovascular form

Neovascular AMD (NV-AMD), also commonly called “wet” AMD, is defined as AMD with the presence of choroidal neovascularization (CNV). It may be accompanied by associated manifestations such as pigment epithelium detachments (PED), retinal pigment epithelium tears, fibrovascular scarring and vitreous hemorrhage.⁴³

CNV can appear as a white-yellow elevation of tissue in the deep retina, with associated neurosensory detachment of the retina due to sub-retinal fluid. Intraretinal fluid and associated hemorrhages are also frequent. Frequently, the evolution of CNV leads to the formation of fibrovascular glial formations known as disciform scar. The scars can be accompanied by massive hemorrhages and lipid exudation, as seen in figure 10.

Figure 10



A. Multicolor picture of a disciform scar.

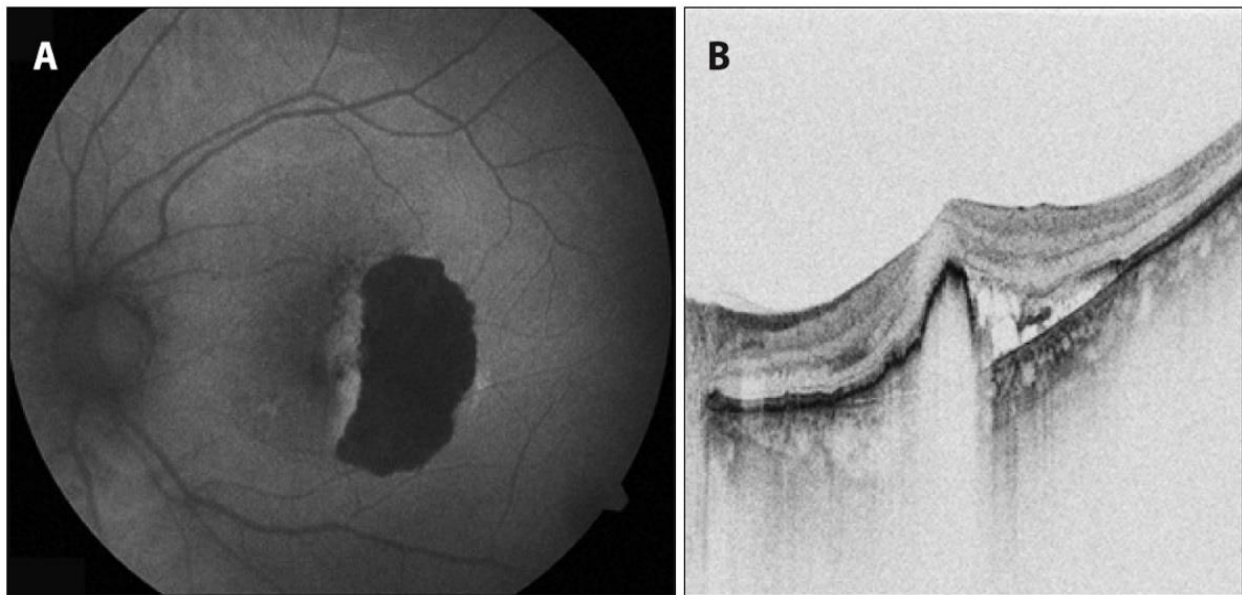
The lesion appears yellowish and elevated. Focal intraretinal hemorrhages are also visible. The lesion is surrounded by scattered drusen.

B. Spectral coherence tomography of the same lesion. A CNV is visible.

Retinal PED are well demarcated dome shaped elevations of the RPE, they can be either serous (filled with serous semi-transparent fluid), drusenoid (filled with drusenoid material) or fibrovascular (underlying a choroidal fibrovascular membrane) The presence of a PED does not always associate with a CNV.

A frequent complication of NV-AMD is the formation of RPE tears, which are breaks of the RPE frequently located at the edges of a PED. After the tear, the free edge RPE rolls and retract, with a characteristic morphology (figure 11).

Figure 11



Multimodal imaging of RPE rip. A: Autofluorescence. A large kidney-shaped hypoautofluorescent area is seen correspondent to the RPE rip. **B. Optical coherence tomography.** The RPE is scrolling and retracting.

1.3 ROLE OF THE CHOROID IN THE PATHOGENESIS OF AGE RELATED MACULAR DEGENERATION

1.3.0 Vascular model of Age Related Macular Degeneration

Although there is strong evidence suggesting that the innate immune system is implicated in the mechanisms that lead to AMD, a primary vascular component has been proposed as contributing to AMD pathophysiology. Over the last years, the vascular model of AMD has growing in importance, with multiple histopathologic studies supporting this evidence.⁴⁵⁻⁵²

This vascular model proposes an increase in choroidal vascular resistance due to a decrease in ocular compliance, in turn caused by the increased rigidity of the sclera in the ageing eye. This reduction in choroidal perfusion, together with the increased hydrostatic pressure, decrease the processing of outer segment lipid by the RPE and, therefore reduce also the clearance of the lipoproteins. Such metabolic alterations lead to the clinical characteristics of the disease, including drusen, pigmentary changes, and GA.⁵²

Progression to NV-AMD and CNV development involve also angiogenic factors such as the vascular-endothelial growth factor (VEGF), which is overexpressed by hypoxia and ischemia.⁵²

Several studies indicate that there are significant abnormalities in the choroidal vasculature and choroidal blood flow in AMD.⁴⁵⁻⁵²

Using color Doppler imaging, Friedman et al. found reduced blood flow and increased resistance in the central retinal artery and the posterior ciliary arteries in a mixed group of AMD patients, if compared with age-matched control subjects without AMD.⁵⁰

In later studies, this finding was confirmed and extended upon by other groups using alternative imaging techniques, such as fluorescein angiography. Using this imaging modality, Prünke and Niesel first reported increased mean times for arterial, capillary, and venous filling, and reduced capillary density in patients with AMD, indicative of reduced choroidal blood flow.⁵³

More recently, Ciulla et al. showed delayed and heterogeneous filling of the choroid of AMD patients, employing a technique based on scanning laser ophthalmoscope indocyanine green angiography.⁵⁴

Abnormal choroidal blood flow in AMD has also been suggested based on laser Doppler experiments,^{55,56} pneumotometry⁵⁷ and interferometry.⁵⁸

1.3.1 The aging choroid

The choroid and its vasculature undergo various changes during normal aging, and these changes often become more severe in eyes with AMD. However, it is not yet clear whether such changes are a cause or an effect of AMD pathology.

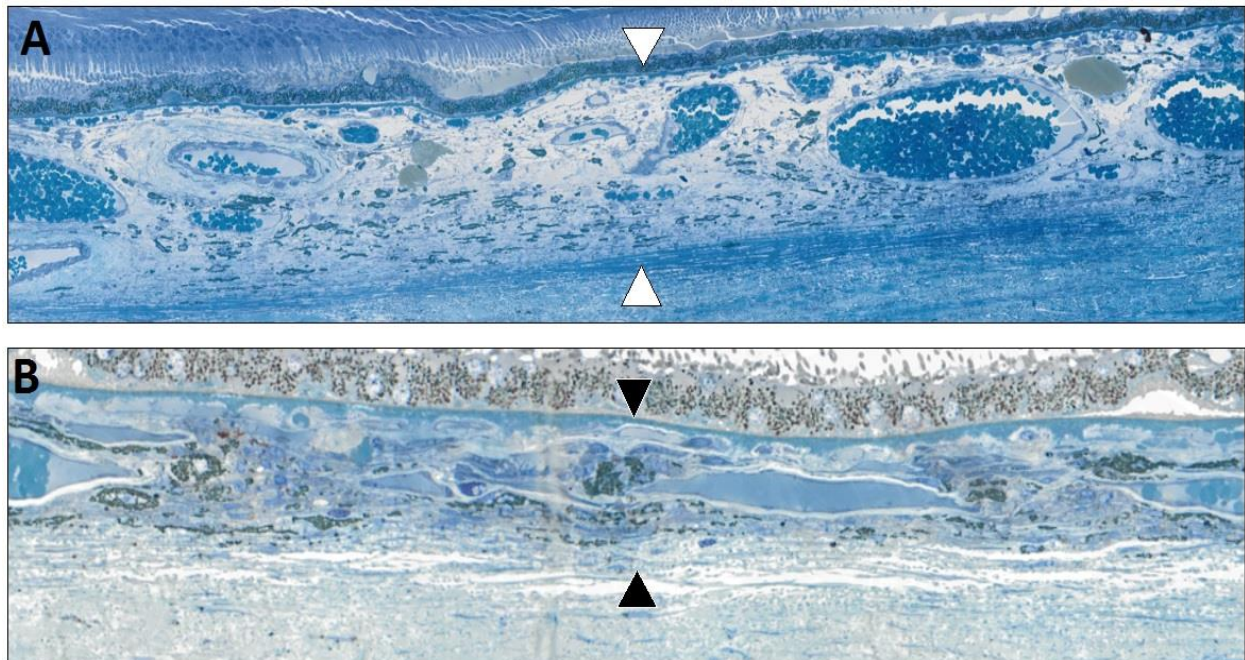
Choroidal thickness has been shown to be dynamic, with rapid changes of up to 100 μm occurring within hours of a myopic defocus stimulus in chickens.³⁹

Diurnal fluctuations of choroidal thickness up to 40 μm have been shown in chickens, being the choroid thickest at night and thinnest during daytime.³⁹

Reversible changes in choroidal thickness in humans are much smaller in magnitude, as shown by Brown and Usui, but still subject to circadian variations.⁵⁹

However, the aging choroid seems to undergo a significant and, more importantly, permanent decrease in choroidal thickness (figure 12).

Figure 12



Photomicrograph pictures of the choroid, same magnification. A: 60 years old female. The choroid has a normal thickness (white arrows); the vessels of the Haller's layer have a good lumen. **B. 90 years old male.** The choroid appears significantly thinner if compared to A (black arrows). The morphology of the choroidal vessels is remarkably compromised, with significant atrophy and reduction of the lumen diameters.

Using swept-source OCT, Wakatsuki et al. found that total choroidal thickness decreases with age, with the thickness of the choroid beneath the fovea decreasing by approximately 3 μm per year.⁶⁰

A decrease in choroidal thickness has been shown to be a risk factor for CNV development, as reported by Grunwald et al. They discovered a significant association between decreased circulation within the choroid and increased risk for wet AMD.⁶¹ This

confirmative data implicates ischemia in CNV formation, and provide evidence for the importance of decreased choroidal blood flow in disease progression.

Moreover, various histological studies showed the association between decrease in choriocapillaris density and the increase in the number of ghost vessels.⁶² This suggests that the difference in vascular density are due to loss of endothelial cells, not innate variability in vessel density.

Recent OCT studies demonstrated that eyes with GA have a thinner choroid than age-matched controls or those with early AMD.⁶³

In biochemical studies of donor choroids, thin choroids were found to have higher levels of tissue inhibitor of metalloproteinase-3 (TIMP3), whereas thicker choroids exhibit higher levels of serine proteases, with corresponding shifts in the balance between fibrillar collagen and ground substance in the choroidal stroma. Altered abundance and/or function of proteases or their inhibitors may be an important factor in choroidal thinning and AMD pathogenesis.⁶²

1.4 IMAGING THE CHOROID

Due to its peculiar localization between the retinal pigmented epithelium and the underlying sclera, the choroid is challenging to visualize.

The retinal pigmented epithelium is a tissue with high concentration of melanin and pigment, which can block imaging modalities based on fluorescence and light reflection.

Various imaging techniques have been employed over the years to visualize this peculiar tissue of the eye.

1.4.0 Fluorescein angiography

Fluorescein is a manufactured organic compound and dye. It is stimulated by blue light with a wavelength between 465 and 490 nm and emits a green light with a peak emission between 520 and 530 nm and a curve extending to approximately 600 nm.

Angiography with fluorescein dyes has been widely used for decades in the imaging of retinal disorders, but has very limited use in choroidal imaging (figure 13, A). In fact, both the excitation and emission spectra from fluorescein are blocked in part by the pigment of the RPE. Moreover, the fenestrated nature of the capillaries of the choriocapillaris causes leakage of fluorescein, impeding sufficient delineation of the choroidal anatomy.

1.4.1 Indocyanine green angiography

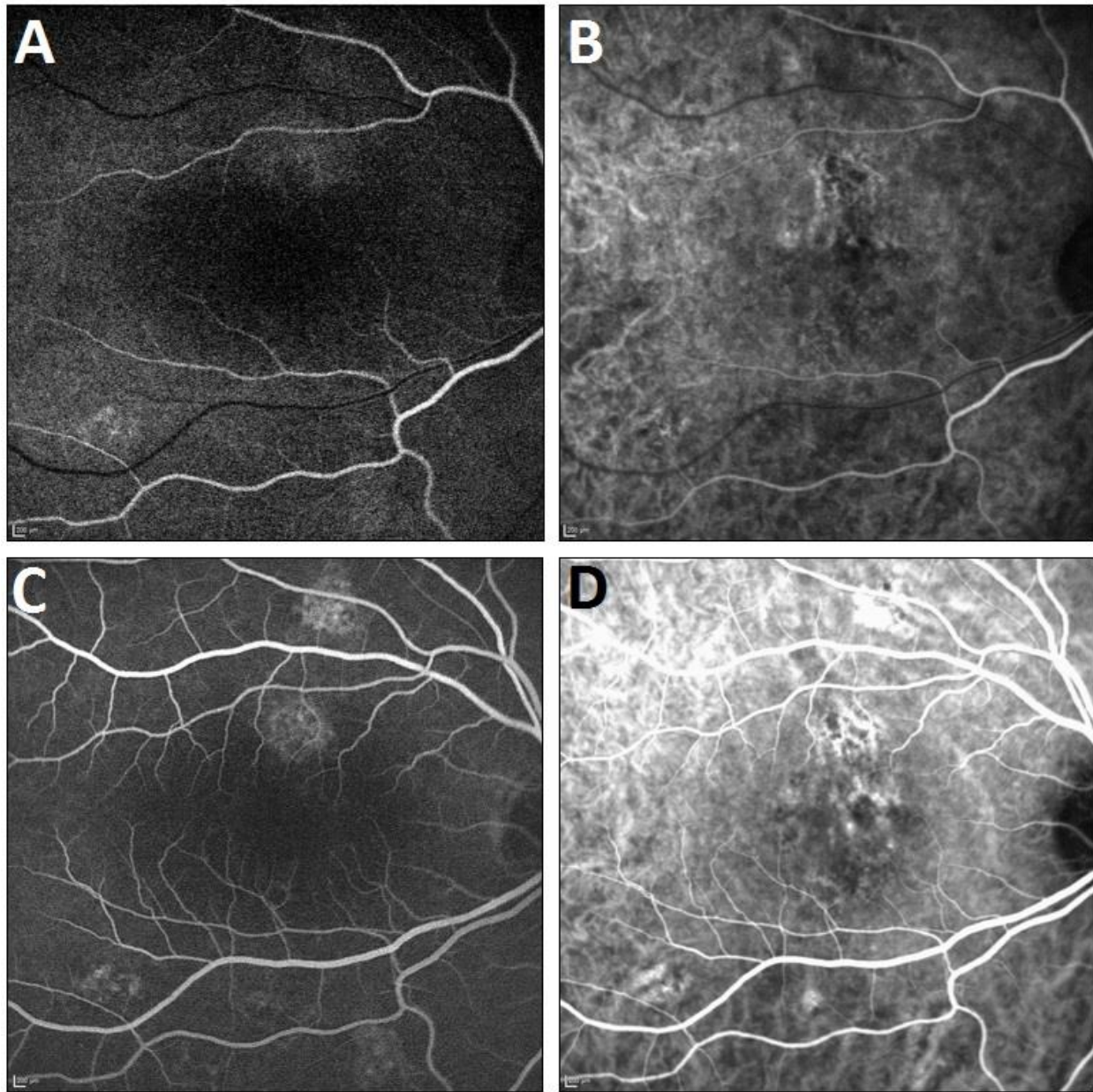
Indocyanine green (ICG) is a cyanine dye widely used in medical diagnostics and particularly useful in the imaging of the choroid (figure 13, B). ICG absorption peak is between 790 and 805 nm, a longer wavelength if compared to fluorescein. Such characteristics allow ICG fluorescence to better penetrate highly pigmented tissues such as the RPE.

Moreover, ICG is 98% plasma protein bound and thus is less likely to leak from the normal choroidal vessels.

During the earlier phases of ICG angiography, the choroidal vessels are clearly delineated, but overlaps phenomena between vessels of different layers make difficult to precisely localize them. This type of angiography allows the dynamic evaluation of the choroidal circulation real-time.

The disadvantage of ICG is that it is an invasive procedure, as the dye needs to be injected intravenously to the patient in order to reach the choroidal circulation. The toxicity of the compound is low, but the administration is not free of risks, especially during pregnancy.

Figure 13



Comparison of fluorescein and indocyanine green angiography in the same eye.

A, B: Early laminar phase of the angiogram. Differently to fluorescein (A), which is blocked by the RPE, indocyanine green (B) allows the visualization of the choroidal vascular network. **C, D. Late phase of the fluorescein.** Also in late phase choroidal vessels are seen beneath the retina with indocyanine green (D) and not with fluorescein (C).

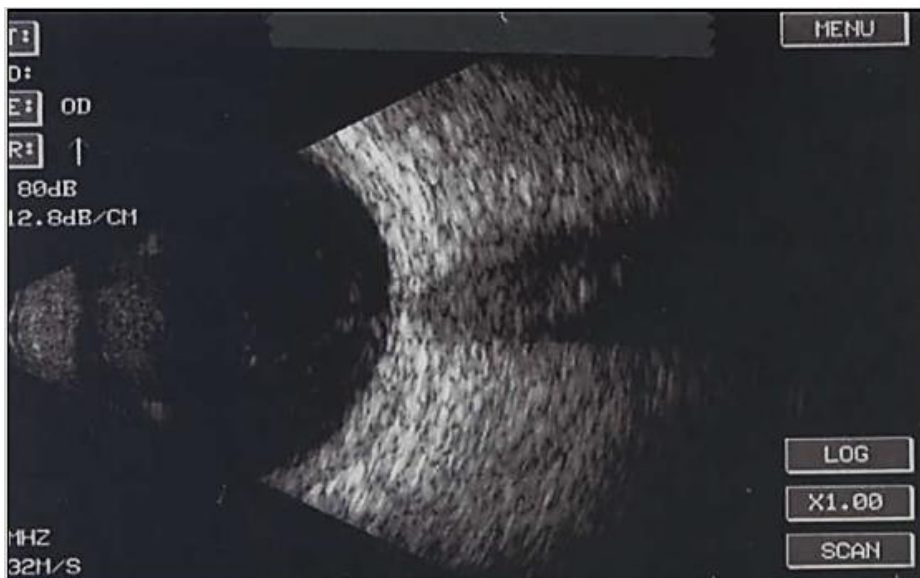
1.4.2 Ultrasonography

Contact B-scan ultrasonography technology uses the vibration of a piezoelectric crystal located into a probe to reconstruct images of the eye.

The vibration of the crystal is stimulated by an electrical current, and produces sound waves which are reflected by intraocular structures, and detected by the same crystal. The reflected sound waves vary in strength according to the position of the structures into the eye, with deeper tissues (such as the choroid) producing weaker reflections.

This technique provides low resolution images of the choroid, it is very useful to detect gross thickening of the choroid, such as in tumors. However, the low resolution makes this imaging modality not reliable to measure precisely smaller variations in choroidal thickness (figure 14).

Figure 14



B-Scan.

The resolution of the image is insufficient for reliable choroidal thickness measurements.

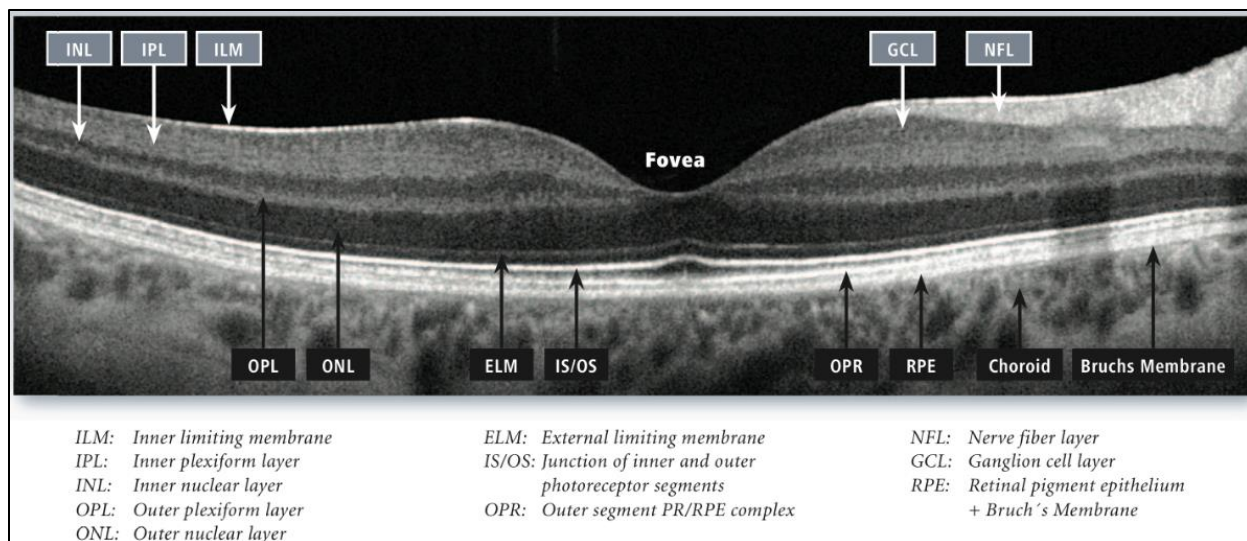
1.4.3 Spectral-Domain Optical Coherence Tomography

Spectral-Domain Optical Coherence Tomography (SD-OCT) is a non-invasive, high resolution, high speed imaging technique which is becoming the gold standard in the diagnosis of many retinal and choroidal disease (figure 15).

SD-OCT uses near-infrared light to capture images in micron-scale resolution. It is based on the principles of *interferometry*, a technique in which electromagnetic waves are superimposed to extract information.⁶⁴

Differently from older time-domain machines, newer SD-OCT uses Fourier transform to decompose a signal into the frequencies that make it up. This technology can produce useful information from all depth levels. However, the sensitivity of SD-OCT decreases at increasing depths. This translates in lower resolution of deeper tissues such as the choroid.⁶⁴

Figure 15



SD-OCT cross-sectional scan of a normal macula. The different retinal and choroidal layers are labeled.

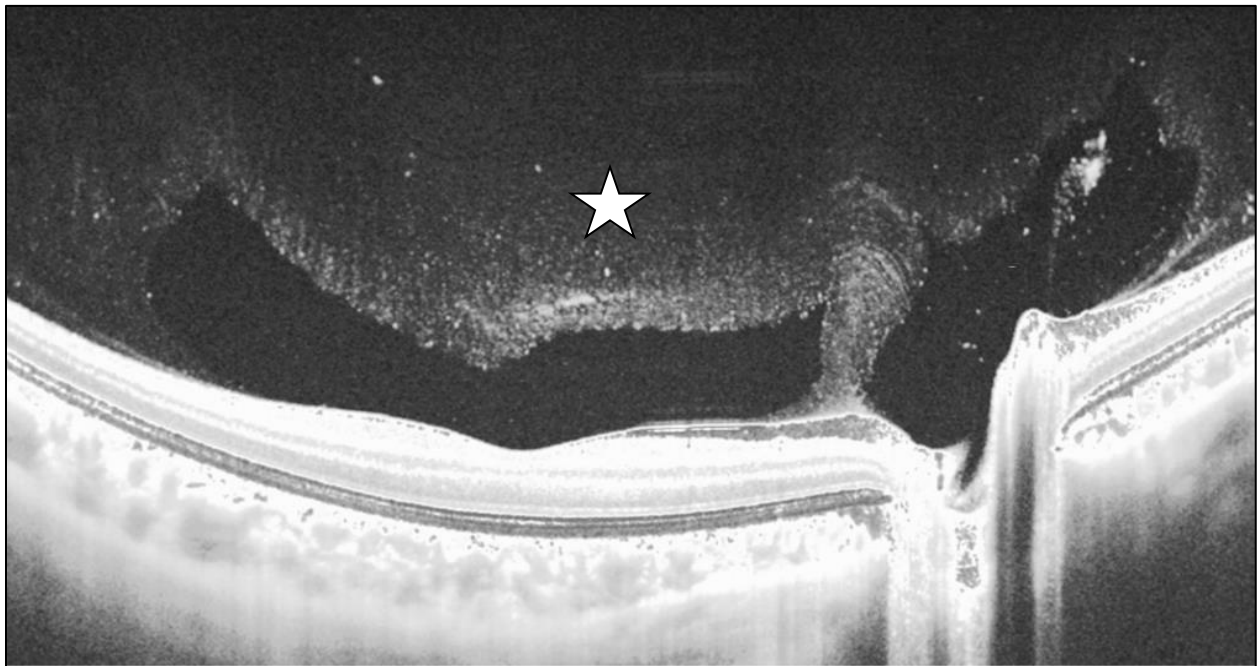
1.5 IMAGING THE CHOROID WITH SD-OCT

1.5.0 Enhanced Depth Imaging

In 2009, in a landmark paper Margolis and Spaide described a novel SD-OCT imaging technique named enhanced depth imaging (EDI) which provides detailed and high resolution pictures of the choroid.¹

In normal SD-OCT settings, the peak of signal, in other words the point in which the images reach the highest resolution, is normally placed at the level of the vitreo-retinal interface. This is because the vitreous is a quasi-transparent tissue, and to visualize it high levels of sensitivity are needed (figure 16).⁶⁴

Figure 16

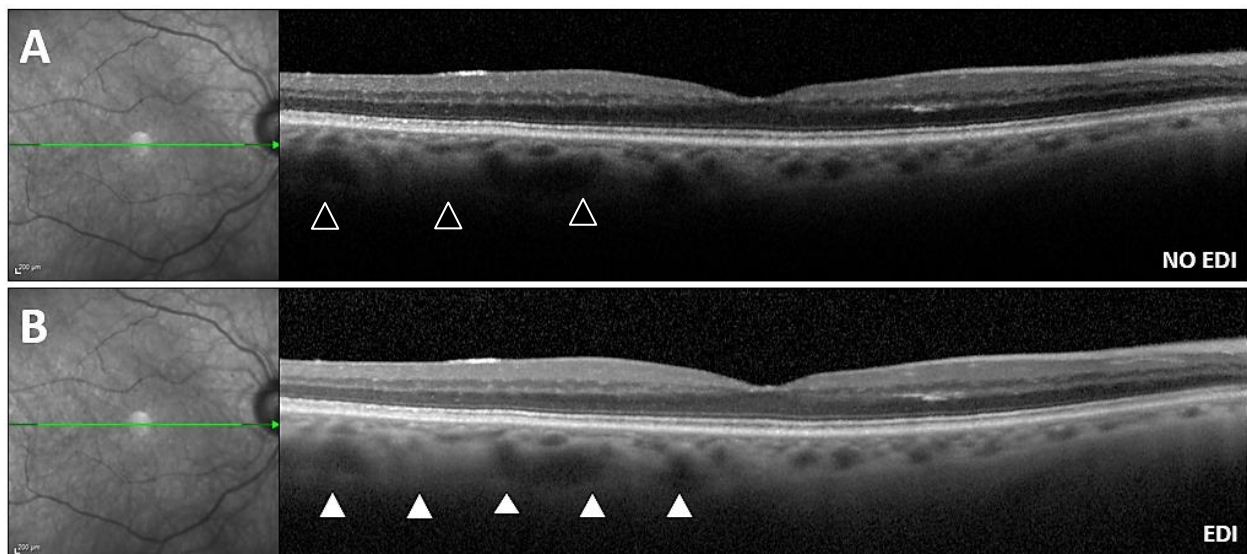


Normal SD-OCT settings. The peak of sensitivity is placed at the level of the vitreous (white star).

However, placing the peak of signal in such position does not allow to see the choroid properly, as deeper structures are darker in the SD-OCT images due to decrease sensitivity (figure 17, A).

In EDI settings, the peak of sensitivity is placed in the inner sclera, so as deeper structures and the choroid can be seen (figure 17, B).¹

Figure 17



A: SD-OCT without EDI module. The outer border of the temporal choroid is darker and its margins cannot be identified precisely (black arrows). **B: SD-OCT with EDI module.** The peak of sensitivity is moved to the inner sclera, the temporal choroid become visible and its outer margins are easily identified (white arrows).

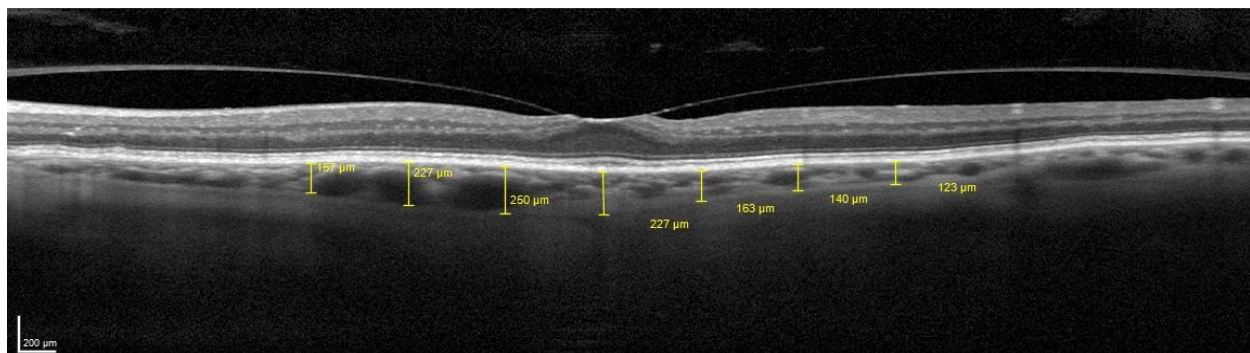
While in earlier versions the user had to manually set the SD-OCT machine to obtain inverted EDI images,¹ now almost all commercially available SD-OCT platform can automatically perform EDI OCT without any manual set up by the user.⁶⁴

The inconvenience of EDI imaging is that the vitreous is not properly visualized, and to do so is it necessary to take another SD-OCT scan with the peak of sensitivity placed at the vitreo-retinal interface.

1.5.1 Choroidal thickness measurements using EDI SD-OCT imaging

The measurement of the choroidal thickness can be performed manually, using the “caliper” function incorporated in every commercially available SD-OCT platform. The inner limit of the choroid is located at the junction between the choriocapillaris and the Bruch membrane, while the outer limit is located at the transition between choroid and sclera. Both inner and outer limits are hyperreflective. A straight line is traced with the caliper from the inner to the outer limit of the choroid, perpendicularly to the retinal pigment epithelium line, in the point in which the operator wants to measure the choroidal thickness (figure 18).

Figure 18



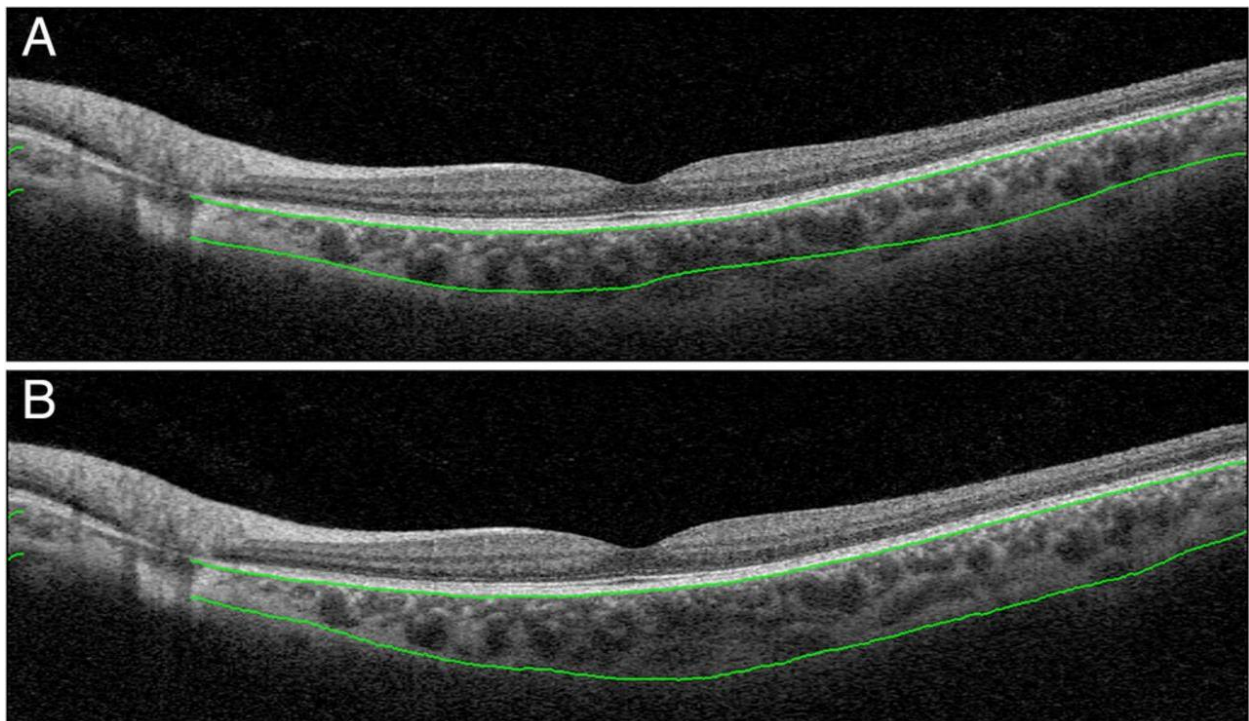
Manual measurement of choroidal thickness. Straight lines are traced with the “caliper” function of the Heidelberg Spectralis platform.

These measurements are punctual, and may vary considerably as the thickness of the choroid is not uniform. Averaging the mean choroidal thickness can be done by arithmetic mean between various punctual measurements.

Recently, various experimental software have been implemented in SD-OCT platform, with the capability of segment automatically the whole choroid, extrapolating the average choroidal thickness without the need of manual measurements (figure 19 A,B). However, the reproducibility and sensitivity of such measurements is object of debate.⁶⁵⁻

67

Figure 19



Automatic segmentation of the choroid. A: incorrect segmentation. The green line does not follow correctly the outer margin of the choroid. **B: correct segmentation.** The green line follows correctly the outer margin of the choroid.

1.5.2 Reproducibility of choroidal thickness

The reproducibility of sub-foveal CT manual measurements has been evaluated in several studies. There is a very good inter-system, inter-observer, and inter-visit reproducibility. The inter-observer reproducibility is excellent between different SD-OCT platforms such as the Cirrus OCT (Carl Zeiss), Spectralis OCT (Heidelberg engineering), Optovue RTVue (Optovue Inc) and TopCon SD-OCT 2000 (TopCon Corp.).⁶⁴

The mean difference between choroidal thickness measurements between two graders was 2 μ m in a study from Tan et al.⁶⁸ This value is considerably less than the diurnal fluctuations of choroidal thickness in healthy eyes.

Recent publications showed that automated software can achieve fast, reliable, and objective measurements of choroidal thickness and volume. The advantage of automated software is that they are normally faster and do not require high operator skill levels.⁶⁹

1.5.3 Normal choroidal thickness and its variations

The choroidal thickness is characterized by an extreme variability among individuals. In a large population-based study, normal choroidal thickness varied between 8 and 854 μ m.¹² This makes difficult the creation of a normative database and the definition of “normal” versus “abnormal” thickness of the choroid.

Numerous studies investigating choroidal thickness in healthy groups of patients have been published. Margolis and Spaide were the first to investigate the choroidal

thickness in a population of healthy individuals and found a mean value of choroidal thickness of 287 μm .¹

Increasing age was significantly associated with decreasing CT, with CT decreasing of approximately 16 μm for each decade of life.¹

Subsequent reports found variable values of CT in normal patients. For instance, Ikuno et. al found normal CT to be 354 μm in a group of non-myopic Japanese patients. In their study the yearly decrease of CT was comparable to that of Margolis and Spaide, being of 14 μm .⁷⁰

The correct visualization of the chorio-scleral interface is seminal to obtain reliable measurements. If the outer limit of the choroid is insufficiently visualized with SD-OCT, the measurements can be biased.

Such extreme variability in CT makes inter-studies comparisons complicated and unreliable. The definition of “normal” is not universal in choroidal thickness, and varies from study to study. Moreover, the choroidal thickness may be influenced by a broad spectrum of factors such as age, axial length, systemic blood pressure, ocular perfusion pressure, diurnal fluctuations, smoking, anterior chamber depth, lens thickness, corneal curvature, obstructive sleep apnea syndrome, body mass index, use of phosphodiesterase inhibitors, and others.¹²

CT is also asymmetric, as first shown by Margolis and Spaide. Within the posterior pole, the choroid is thicker at the fovea and thinner nasally to the fovea.¹ The temporal choroid is thicker than the nasal choroid but thinner than the sub-foveal choroid.

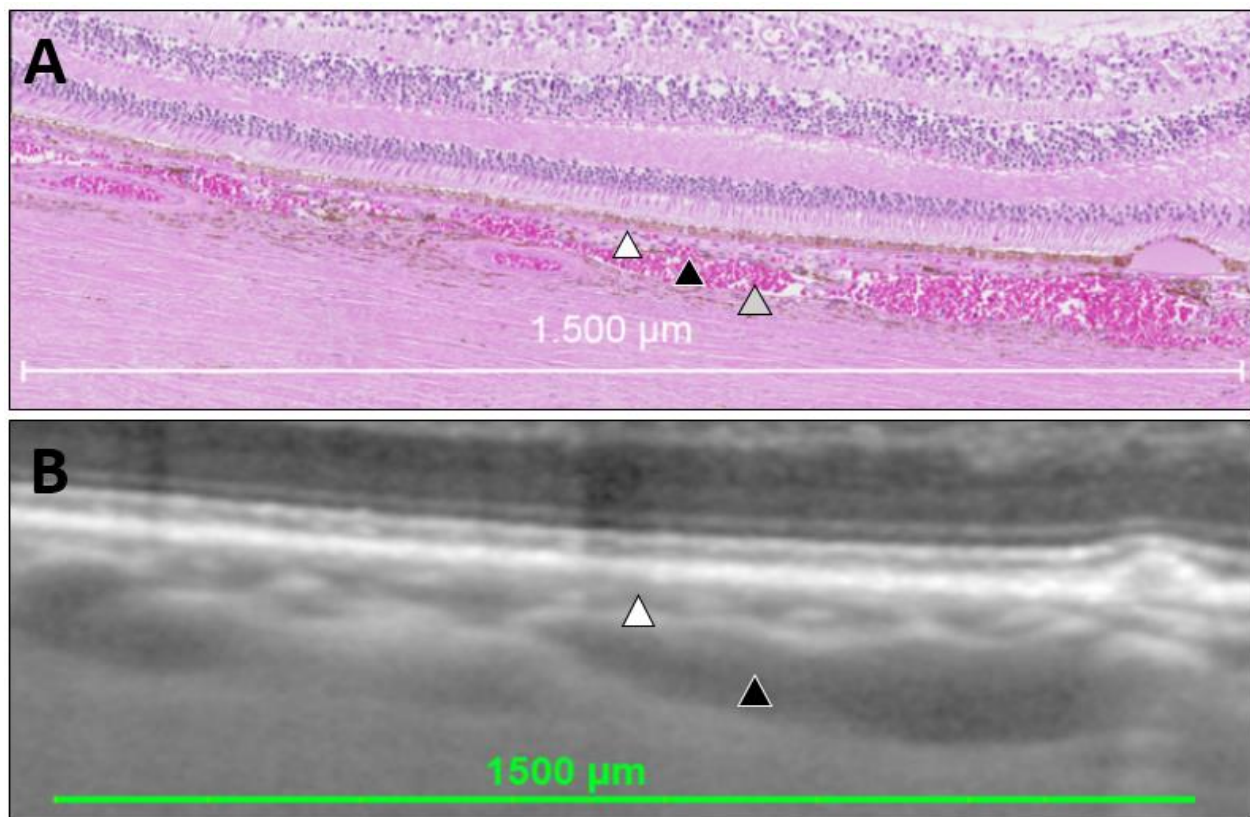
Even measuring the choroid in both eyes of the same patient, significant differences have been shown. For example, Ruiz-Medrano et al. reported significant

differences in nasal CT between left and right eye of healthy subjects.⁷¹ Similarly, Chen et al. and Kang et al. described discrepancies in subfoveal CT in normal populations.^{72,73}

1.5.4 Qualitative analysis of the choroid with EDI SD-OCT analysis

EDI SD-OCT imaging allowed to study in-vivo the morphology of the choroid in a quick, easy and non-invasive way (figure 20, A,B).

Figure 20



Comparison of histologic (A) and SD-OCT EDI imaging of the choroid (B). A. Choriocapillaris (white arrow), Sattler's layer (black arrow) and Haller's layer (grey arrow) are visible. B. Only Sattler's and Haller's layers (white and black arrows) are identifiable.

The first choroidal layer, the choriocapillaris, cannot be visualized in detail with SD-OCT, but some authors believe that the hyperreflective areas below the Bruch membrane may represent a cross section of the capillaries. The dimensions of the small capillaries of this layer has been estimated around 30-40 μ m in histologic specimens, a value comparable with the lumen of the hyperreflective foci, which is around 50 μ m.

The identification of the transition zones between choriocapillaris, Haller's and Sattler's layers is challenging, as there are no clear boundaries between them.

Esmaeelpour et al. presented a novel automated segmentation software capable of differentiating Haller's and Sattler's layers; However, the automated segmentation was not accurate, and needed manual control for by an experienced observer.⁷⁴

2 MATERIAL AND METHODS

2.0 Study design, participating centers, study population

A retrospective, multicenter, observational chart review of consecutive patients diagnosed with non neovascular (NNV) AMD in one eye and with neovascular (NV) AMD in the fellow eye and evaluated by three retina specialists (Marta Suarez de Figueroa, Jean Pierre Hubschman, and Francesco Bandello) at the Ramon y Cajal University Hospital (Madrid, Spain), the Stein Eye Institute, University of California Los Angeles (USA), and the San Raffaele Hospital (Milan, Italy) between January 2014 and January 2015 was carried out.

This study was approved by the institutional review boards of the Ramon y Cajal University Hospital, the University of California Los Angeles, and the San Raffaele Hospital. Cases were identified by a medical billing record search, using the international statistical classification of diseases and related health problems, ninth revision (ICD-9) diagnosis code 362.50 for AMD.

All patients underwent a complete ophthalmological examination including best-corrected visual acuity (BCVA) assessment, slit lamp bio-microscopy and fundus examination by an experienced retina specialist (Marta Suarez de Figueroa, Jean Pierre Hubschman, Francesco Bandello and David Sarraf).

BCVA was reported in Snellen fraction and converted in the Logarithm of the Minimum Angle of Resolution (LogMAR) values for statistical analysis.

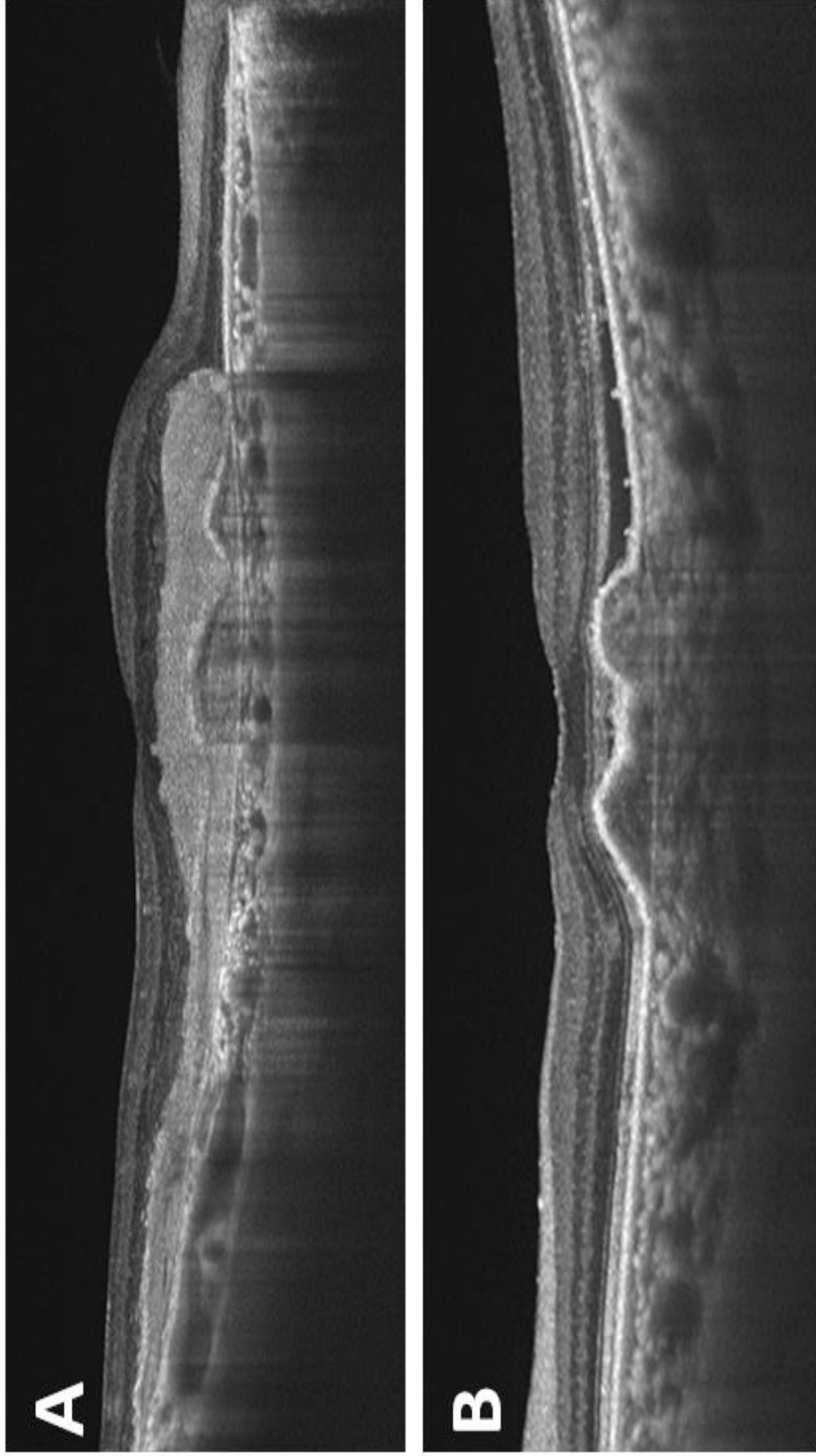
2.1 Exclusion criteria

Exclusion criteria included a refractive error equal to or greater than ± 3 diopters, anisometropia (defined as difference in refractive error between the two eyes of more than 1.00 dioptre in any meridian), history of glaucoma, diabetic retinopathy, central serous chorioretinopathy, polypoidal choroidal vasculopathy, pachychoroid neovascularopathy, retinal angiomatous proliferation, uveitis or any other intraocular inflammation, and any intraocular surgery with the exception of uncomplicated cataract extraction.

2.2 Imaging acquisition

In all cases, EDI, multicolour, infrared and fundus autofluorescence (FAF) images were obtained with the Spectralis HRA-OCT (Heidelberg Engineering GmbH, Heidelberg, Germany) and reviewed with the Heidelberg Eye Explorer (V.1.8.6.0) using the HRA/Spectralis Viewing Module (V.5.8.3.0). To be used for our measurements, choriocapillaris, Sattler's and Haller's layers, as well as the choroid–scleral junction had to be clearly identifiable from the EDI OCT images (figure 21 A,B).

Figure 21



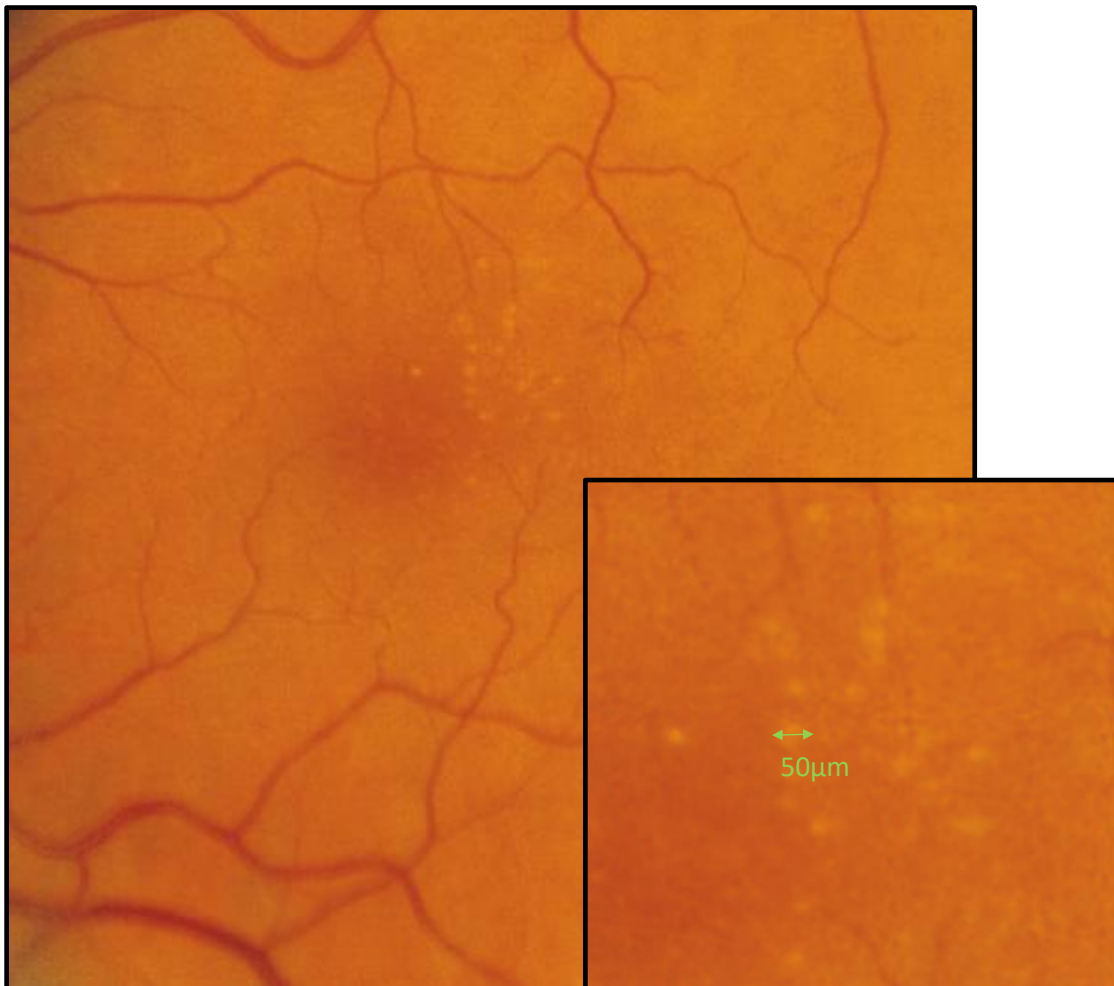
In these two examples of neovascular AMD, Choriocapillaris, Sattler's and Haller's layers, and the choroid-scleral junction are clearly identifiable with the EDI scans.

2.3 Grading technique

NNV AMD eyes were classified into four subgroups according to the Beckman Initiative for Macular Research AMD Classification Committee Meeting:

1. **Normal ageing changes:** eyes with small drusen <61 μm (NNV AMD group 1, Figure 22).

Figure 22



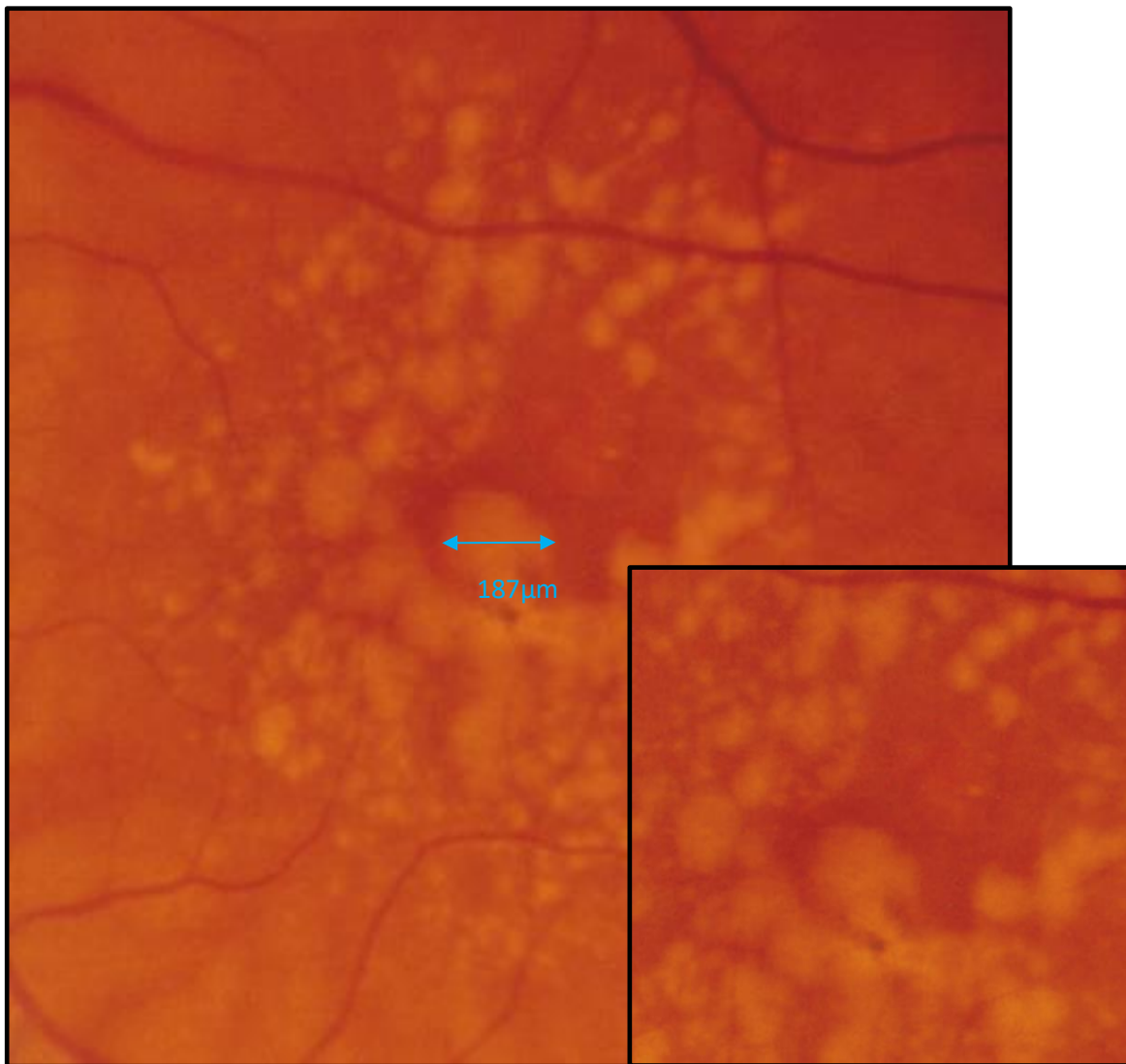
2. **Early AMD:** eyes with medium drusen between 63 and 125 μm without pigmentary abnormalities (NNV AMD group 2, Figure 23).

Figure 23



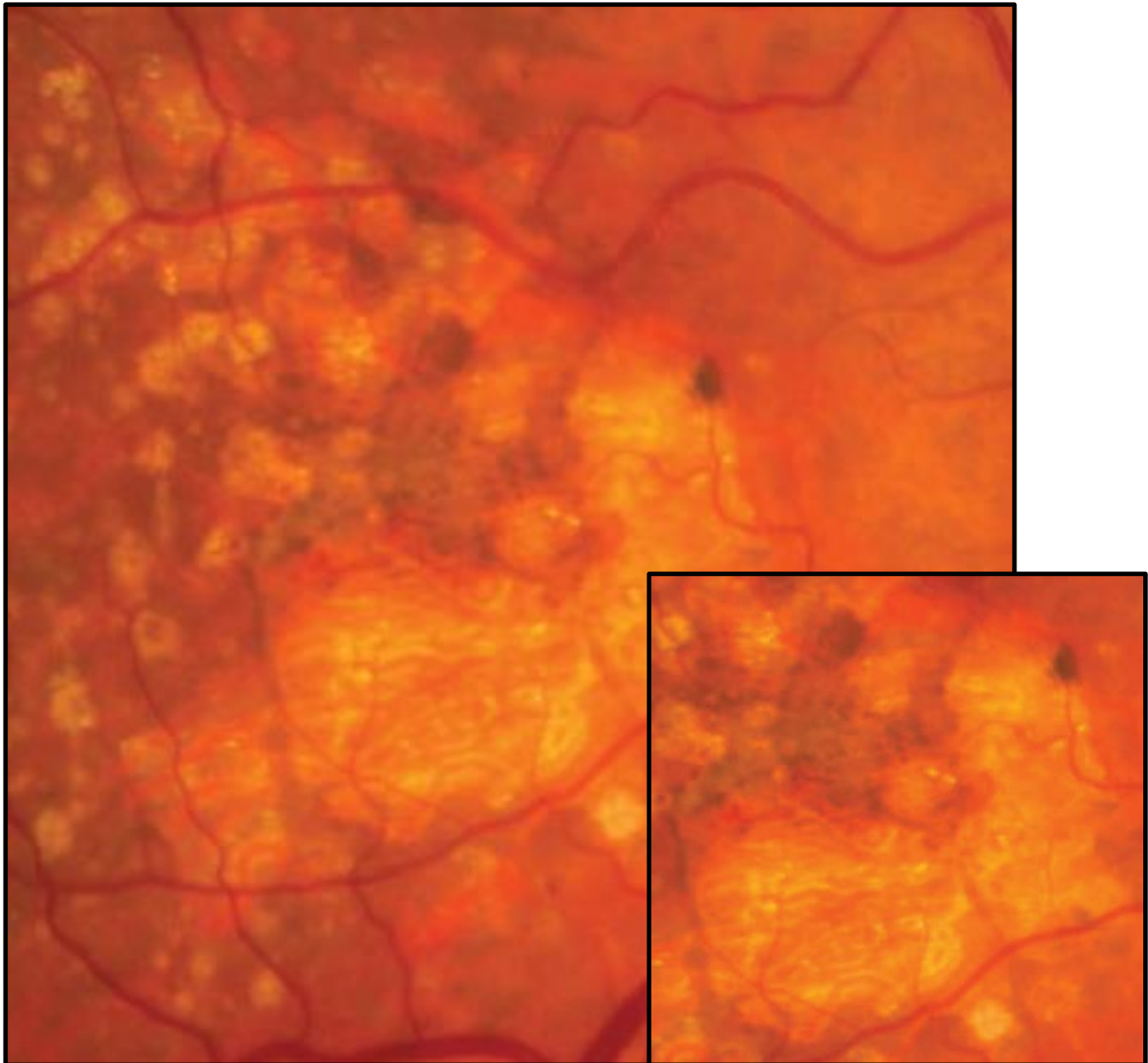
3. **Intermediate AMD:** eyes with large ($>125\mu\text{m}$) or medium drusen associated with pigmentary abnormalities (NNV AMD group 3, Figure 24).

Figure 24



4. **Late AMD:** eyes with geographic atrophy (NNV AMD group 4, figure 25).

Figure 25

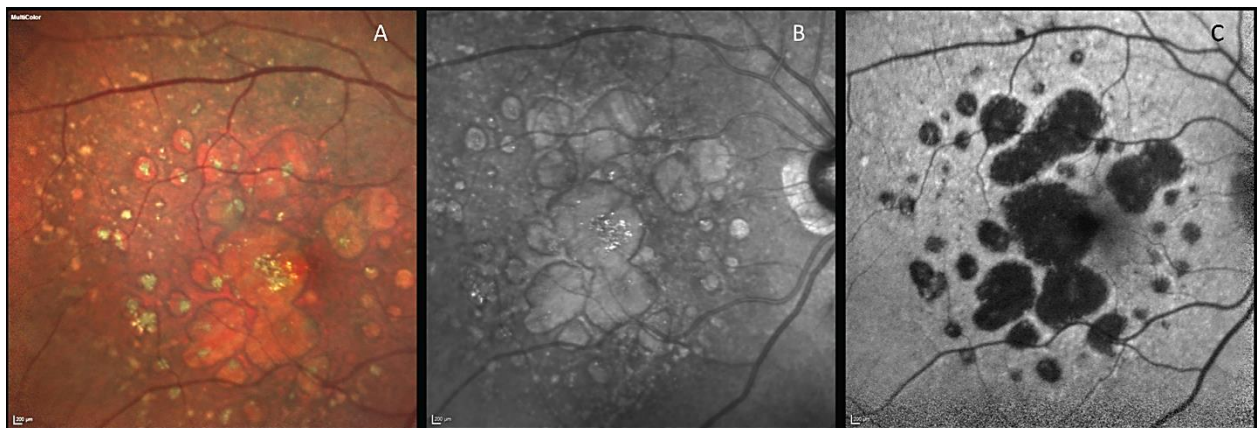


In all cases, grading was conducted by three independent evaluators (Andrea Govetto, Marta Suarez de Figueroa and Luisa Pierro) using multicolor, infrared and FAF images (figure 26).

The diagnosis of geographic atrophy in multicolor images required the presence within the temporal vascular arcades of at least one patch $\geq 250 \mu\text{m}$ of depigmentation with clear borders, partially or completely involving the fovea (figure 26).

On FAF, geographic atrophy was recognized as well demarcated hypoautofluorescent areas corresponding to retinal pigment epithelium defects (figure 26).

Figure 26



Multimodal imaging of geographic atrophy. A. Multicolor picture. Geographic atrophy is seen as multiple patches of depigmentation involving the fovea. **B. Red free picture.** Geographic atrophy patches are lighter if compared to areas without RPE atrophy. **C. Autofluorescence.** Autofluorescence is the gold standard technique to visualize geographic atrophy and its progression. Confluent, well demarcated and hypoautofluorescent patches of RPE atrophy are visible over the posterior pole.

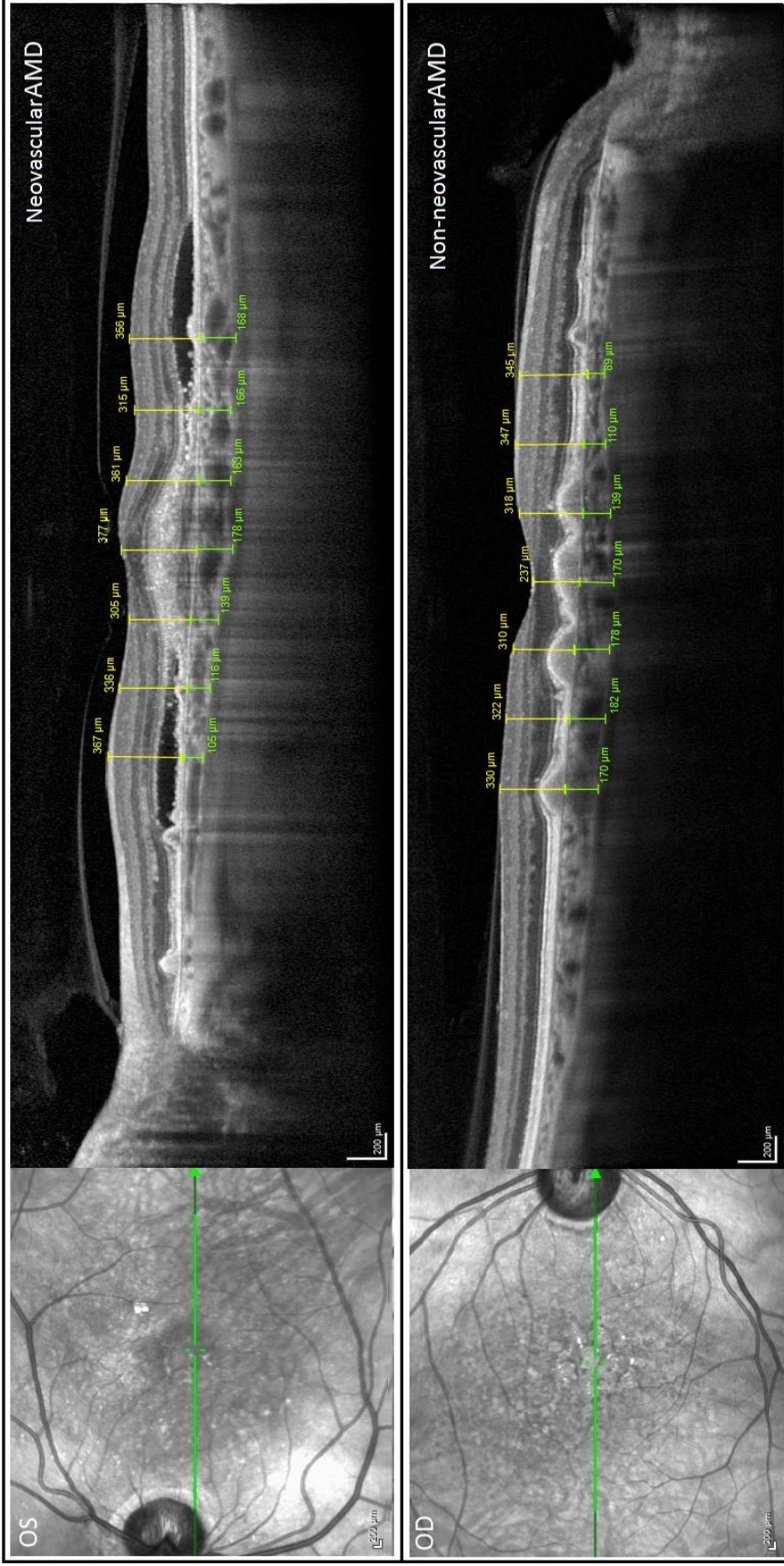
2.4 Choroidal thickness assessment

CT and retinal thickness (RT) measurements were manually performed by two authors (Andrea Govetto and Luisa Pierro) with the 'caliper' function of the Heidelberg Eye Explorer, and revised by at least two independent investigators (Jean Pierre Hubschman, Marta Suarez de Figueroa, David Sarraf and Francesco Bandello).

In all cases, a single high-definition horizontal line centred in the fovea was used for CT and RT assessment. Both CT and RT were measured at the subfoveal region and at 500, 1000 and 1500 μm nasal and temporal to the fovea, as shown in figure 27.

All CT and RT measurements were performed at the last follow-up visit. Mean CT was calculated by arithmetic mean of CT measured at each of the seven locations.

Figure 27



Choroidal and retinal thickness assessment. Both retinal (yellow) and choroidal (green) thickness are measured manually with the caliper function of the Heidelberg spectralis subfoveally and at 500, 1000 and 1500µm nasally and temporally to the fovea.

2.5 Statistical analysis

All the analyses were carried out using the SPSS V.15.0 and R package mgcv (R Development Core Team, available on line at <http://www.r-project.org>).

Descriptive statistics were first calculated for all variables of interest. Mean and SD values were calculated for continuous variables, while frequency and percentage were calculated for categorical variables.

Parametric and non-parametric test (Kruskal-Wallis, analysis of variance, Willcoxon, Student's t-test for paired samples) were used to compare quantitative variables, and χ^2 test was used to compare categorical variables.

Logistic regression was used to evaluate associations of CT with other variables of interest. Spearman's correlation coefficient was used to assess the correlation between CT and RT.

Differences were reported with 95% Cis, while a p value <0.05 was considered statistically significant.

3 RESULTS

3.0 Included study population

After a comprehensive chart review, 322 eyes from 161 patients of which 102 (63.35%) were female and 59 (36.65%) were male, with a mean age of 80.80 ± 8.45 years (range 58–99 years), met the inclusion criteria and were enrolled in the study.

All patients were diagnosed with NNV AMD in one eye and NV AMD in the fellow eye. Of the 161 eyes diagnosed with NNV AMD, 19 were classified as NNV AMD group 1, 33 as NNV AMD group 2, 93 as NNV AMD group 3 and 16 as NNV AMD group 4.

3.1 Best Corrected Visual Acuity

Mean BCVA was significantly higher in NNV AMD eyes compared with NV AMD fellow eyes: 0.33 ± 0.49 LogMAR (Snellen equivalent 20/42) and 0.63 ± 0.53 LogMAR (Snellen equivalent 20/85), respectively ($p < 0.0001$).

When NN VAMD was divided into subgroups, BCVA differences remained significant for subgroups 1, 2 and 3 (NNV AMD group 1, $p = 0.001$; NNV AMD group 2, $p = 0.0001$; NNVAMD group 3, $p < 0.0001$).

3.2 Anti-Vascular-Endothelial Growth Factor Injections

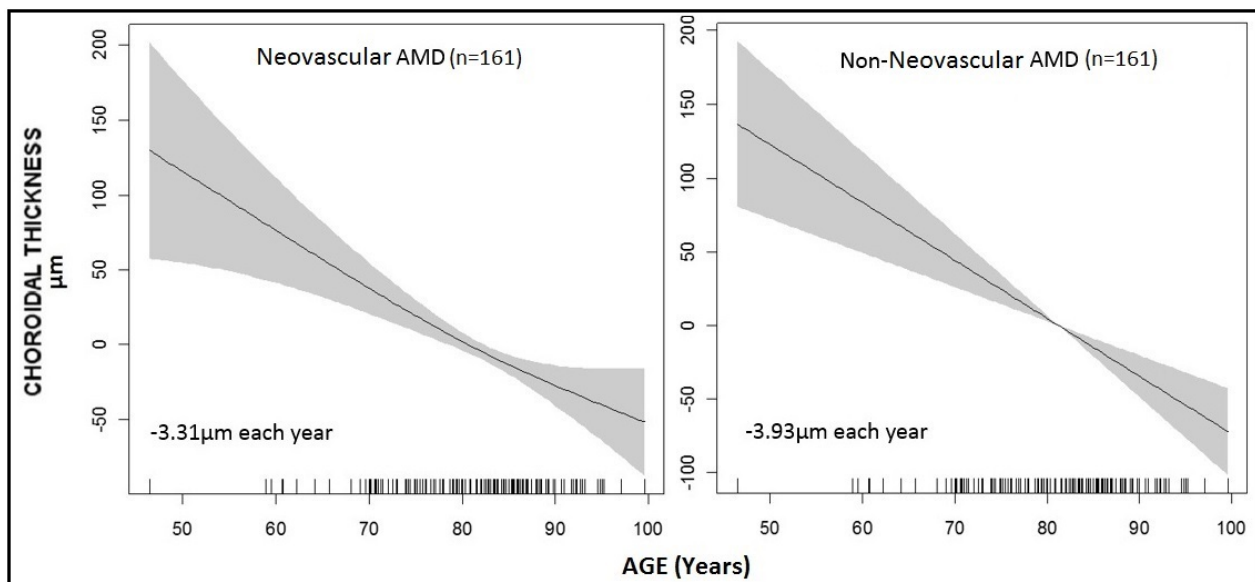
Over the follow-up period, NVAMD eyes received a mean of 7.47 ± 7.7 anti-vascular endothelial growth factor (VEGF) injections (range 0–38), and logistic regression analysis showed no correlation between CT and number of injections ($p=0.95$).

NV AMD eyes received the last anti-VEGF injection at a mean of 4.9 ± 3.9 months before CT measurement (range 1–12 months).

3.3 Associations of choroidal thickness with age

CT was strongly associated with age ($p < 0.001$) in both the NV AMD and NNV AMD groups. Logistic regression analysis showed a linear relationship between age and CT, similar in both groups, with an estimate yearly mean decrease in CT of 3.31 μm in NVAMD and of 3.93 μm in NNVAMD (Figure 28).

Figure 28:

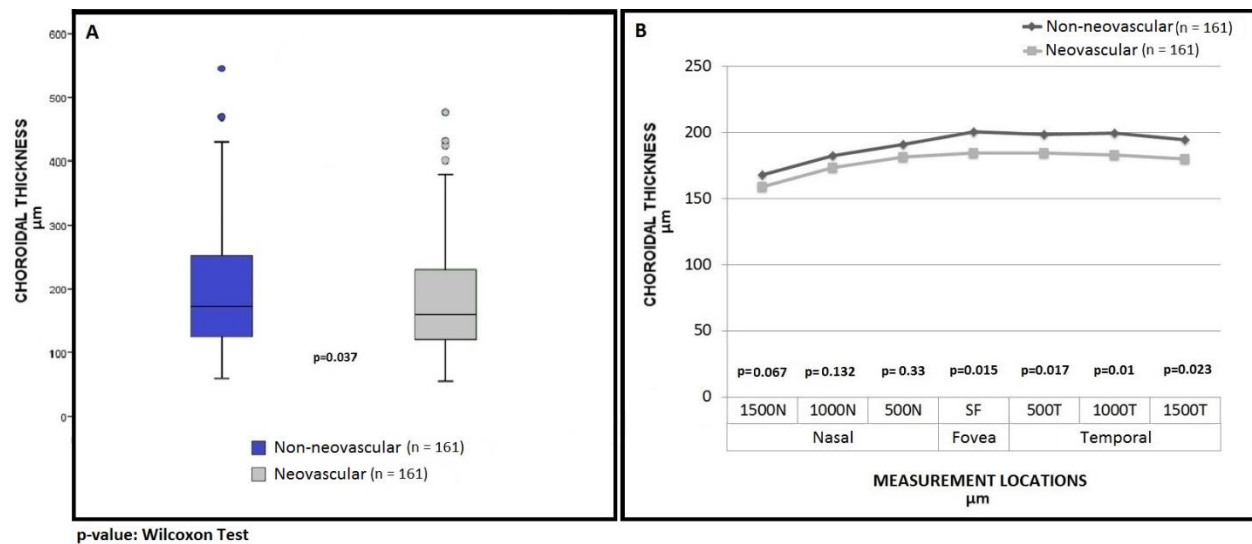


3.4 Choroidal thickness in the study population

Differences in the mean CT between NNVAMD and NVAMD fellow eyes were statistically significant ($p=0.037$, figure 29, A).

When the CT of NNVAMD and NVAMD fellow eyes was compared in all the measured locations, statistical significance was confirmed only in the sub-foveal and temporal areas (figure 29, B and table 1), although CT was lower in the NNVAMD group versus the NVAMD group at every testing position (table 1).

Figure 29



Choroidal thickness evaluation. A: Difference between mean choroidal thickness in non-neovascular versus neovascular AMD. Differences are statistically significant. B: Difference between choroidal thickness in non neovascular and neovascular AMD at any measured location. Differences are statistically significant only in the sub-foveal and temporal areas.

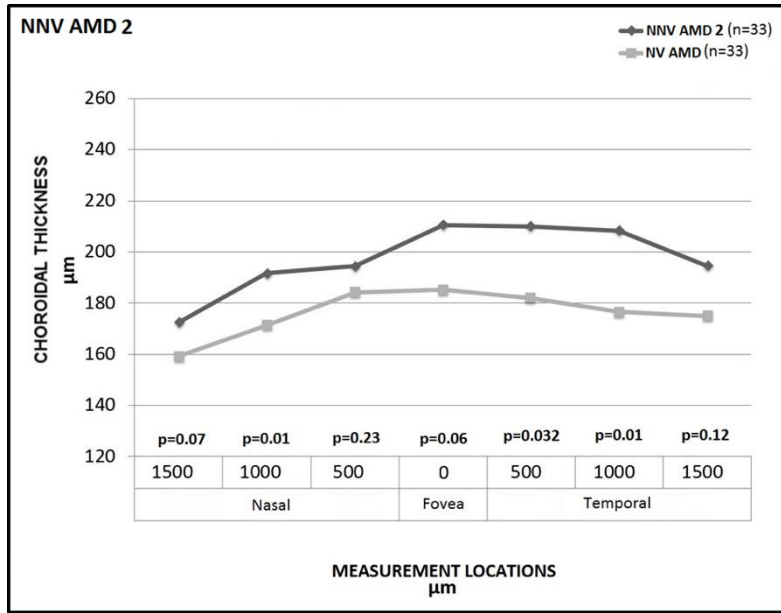
Table 1: Choroidal Thickness in Neovascular (n=161) versus Non-Neovascular (n=161) fellow eyes

Eye	Location	Mean CT (µm)	SD (µm)	p-value
NV AMD	Sub-Foveal	184,36	89,09	0,015
NNV AMD	Sub-Foveal	200,69	109,38	
NV AMD	500µm Temporal	184,53	82,39	0,017
NNV AMD	500µm Temporal	198,47	98,14	
NV AMD	500µm Nasal	181,24	91,30	0,330+
NNV AMD	500µm Nasal	190,78	99,33	
NV AMD	1000µm Temporal	183,14	77,96	0,010
NNV AMD	1000µm Temporal	199,31	91,52	
NV AMD	1000µm Nasal	173,42	90,12	0,132+
NNV AMD	1000µm Nasal	182,45	95,69	
NV AMD	1500µm Temporal	180,09	78,71	0,023
NNV AMD	1500µm Temporal	194,47	80,75	
NV AMD	1500µm Nasal	158,78	89,73	0,067+
NNV AMD	1500µm Nasal	168,02	93,68	
NV AMD	Mean	177,94	81,20	0,037+
NNV AMD	Mean	190,60	91,28	

p-value: Student t test for paired samples. + Wilcoxon Test. **NV AMD:** Neovascular Age-Related Macular Degeneration. **NNV AMD:** Non-Neovascular Age Related Macular Degeneration

Differences in CT between NNV AMD and NV AMD fellow eyes were greater at earlier stages of NNV AMD (NNV AMD groups 1 and 2) as presented in figures 30, 31, 32 and 33.

Figure 30:



Comparison of choroidal thickness between NNV AMD group 1 (normal aging changes) and NV AMD.

The differences are statistically significant at any measured locations with the exception of those taken at 500µm nasally and 1500µm temporally to the fovea.

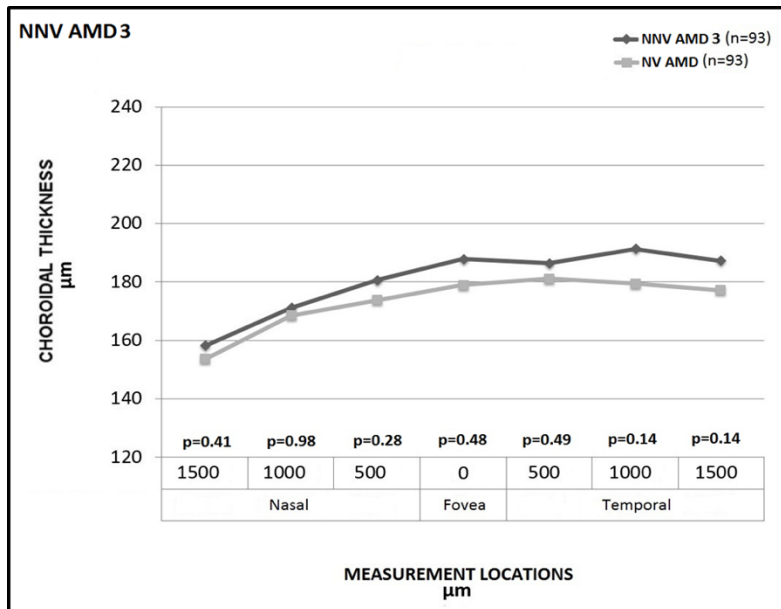
Figure 31:



Comparison of choroidal thickness between NNV AMD group 2 (early AMD) and NV AMD.

The differences are statistically significant only temporally to the fovea.

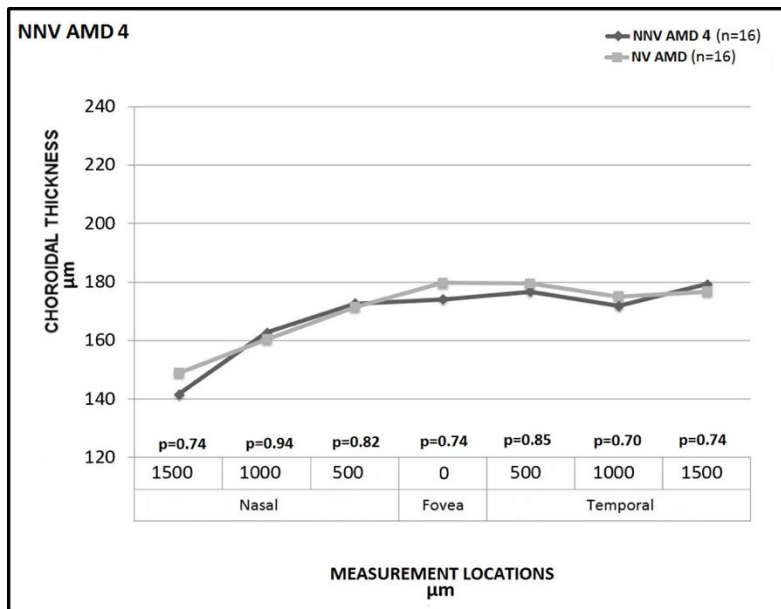
Figure 32:



Comparison of choroidal thickness between NNV AMD group 3 (intermediate AMD) and NV AMD.

The differences are not statistically significant at any measured locations.

Figure 33:



Comparison of choroidal thickness between NNV AMD group 4 (advanced AMD) and NV AMD.

The differences are not statistically significant at any measured locations. Choroidal thickness is almost equivalent in the two groups

A comparison of CT between the four subgroups of NNV AMD was significant with and without age adjustment (table 2).

Table 2: Comparison of Choroidal Thickness between the four subgroups of non-neovascular age-related macular degeneration: Groups 1 vs 2 vs 3 vs 4

p-value**: Anova test, Kruskal-Wallis test. *p-value**: Linear logistic regression model

Location	Not Age Adjusted	Age Adjusted
	p-value*	p-value**
Sub-foveal	0.018	0.026
500µm Temporal	0.027	0.036
500µm Nasal	0.026	0.049
1000µm Temporal	0.06	0.12
1000µm Nasal	0.007	0.037
1500µm Temporal	0.044	0.05
1500µm Nasal	0.006	0.019

Correlations between CT and RT were poor in both NNV and NVAMD, and were not significant at any measured location (table 3).

Finally, in both NV and NNVAMD, no significant association was found between CT and variables such as sex and visual acuity.

Table 3: Correlation between choroidal and retinal thickness in both NV and NNV AMD

Measurement Location	NV AMD (n=161)	NNV AMD (n=161)
Sub-Foveal	r = -0.15 (p=0.082)	r = 0.08 (p=0.35)
500µm Temporal	r = -0.12 (p=0.15)	r = -0.033 (p=0.70)
500µm Nasal	r = -0.12 (p=0.16)	r = 0.04 (p= 0.63)
1000µm Temporal	r = -0.01 (p=0.90)	r = 0.13 (p= 0.13)
1000µm Nasal	r = -0.055 (p=0.52)	r = 0.11 (p=0.20)
1500µm Temporal	r = 0.024 (p= 0.78)	r = 0.20 (p = 0.018)
1500µm Nasal	r = 0.14 (p= 0.092)	r = 0.27 (p = 0.001)

r: Spearman's correlation coefficient

4 DISCUSSION

The role of the choroid may be integral in the development of AMD and other ocular diseases, but the study of this important vascular layer of the eye has been challenging due to its difficult accessibility.⁶⁴

Physiologically, healthy choroid receives about 70% of total eye blood flow, the highest rate of blood flow/unit rate in the human body.²⁵

Its structure consists of an intricate network of blood vessels and extracellular matrix, containing immune system cells, pigment cells, smooth muscle, collagen bundles and intrinsic neurons forming the choroidal parasympathetic plexus.^{26,39}

The functions of the choroid are various: it provides nourishment to the outer layers of the retina and of the optic nerve head, it acts as a thermoregulatory tissue, it absorbs light radiation to reduce scattering, and plays a major role in bulb length adjustment during accommodation.³⁹

Until recently, our knowledge of the choroid was principally the result of post-mortem histologic studies and in-vivo procedures such as ultrasound echography and fluorescein and indocyanine green angiography.

The introduction of EDI OCT capability has provided an easier, more accurate and non-invasive visualization of the choroid with depth resolution that paved the way for a new field of research.¹

However, choroidal thickness (CT) may be influenced by a broad spectrum of factors such as age, axial length, systemic blood pressure, ocular perfusion pressure, diurnal fluctuations, smoking, anterior chamber depth, lens thickness, corneal curvature,

obstructive sleep apnea syndrome, body mass index, use of phosphodiesterase inhibitors, and others.¹²

Age is the most relevant factor influencing CT. Early histologic studies found decreased CT and lower capillary density with age. Ramrattan et al. quantified changes in choriocapillary density and in thickness of Bruch's membrane, the choriocapillaris, and the choroid in 95 unpaired, histologically normal human maculae aged 6 to 100 years and in 25 maculae with advanced age-related macular degeneration. Over ten decades, Bruch's membrane thickness increased by 135%, from 2.0 to 4.7 microns; the choriocapillary density decreased by 45%; the diameter of the choriocapillaris decreased by 34%, from 9.8 to 6.5 microns; and the choroidal thickness decreased by 57%, from 193.5 to 84 microns in normal maculae.⁷⁵

Later, several studies assessed CT with age with EDI-SD OCT. The Beijing Eye Study, a large, cross sectional population study in China, found CT to decrease by 4.1 μm per year of age.¹² Wakatsuki et al. reported similar values in their cross-sectional study of 115 normal Japanese subjects, and found a global decrease of CT of 2.98 μm each year of age.⁶⁰ Another large Chinese population study, the Handan eye study, found that age was positively associated with foveal minimum and central macular thicknesses (per decade increase in age, beta coefficient 3.660 and 2.324, respectively).⁷⁶

The present study confirms the previously published data, and found that age was significantly related with thinner CT, with an estimate yearly mean decrease in CT of 3.31 mm in NVAMD and of 3.93 mm in NNVAMD.

Axial length is also an important confounding factor when analyzing CT. Flores Moreno et al. found CT to decrease by 25.9 μm for each additional millimeter of axial length, being thinner in eyes with high myopia.⁴ The Beijing eye study found that in the

myopic refractive error range of more than 1 Diopter, sub-foveal CT decreased by 15 μm (95% CI, 11.9 –18.5) for every increase in myopic refractive error of 1 Diopter or by 32 μm (95% CI, 37.1–26.0) for every increase in axial length of 1 mm.¹²

While in the present study variations in CT with axial length were not analyzed, we included in our analysis only emmetropic patients or patients in the range of ± 3 Diopters, and we excluded anisometropic patients. Moreover, we compared both eyes of the same patients, using one eye as control of each other. Therefore, the confounding effect of axial length on CT in our study was limited.

Diurnal fluctuations are also an important factor to consider when analyzing CT. In a small study analyzing CT in 12 patients, Tan et. al found a statistically significant diurnal variation in CT, with mean maximum CT of 372.2 μm , minimum of 340.6 μm , and mean diurnal amplitude of 33.7 μm .⁶⁸ Another in-vivo study by Brown et al. used partial coherence interferometry (PCI) to estimate CT and confirmed significant diurnal fluctuations.³³ Kinoshita et. al suggested that there may be significant diurnal variations in the total choroidal area, luminal area but not in the stromal area.⁷⁷ These findings indicate that the diurnal variations in the choroidal area are mainly due to the fluctuations in the luminal area.

In the present study, the confounding effect of diurnal fluctuations was limited, as all patients were examined between 9AM and 12PM.

Other confounding factors such obstructive sleep apnea and use of phosphodiesterase inhibitors were not registered in any of the included patients.

The effect of anterior chamber depth, lens thickness, and corneal curvature was limited as these values have shown good levels of symmetry between both eyes of the same patient.

The present study confirms the correlation between CT and AMD status, and showed a significantly thicker choroid in the sub-foveal and temporal regions in non-neovascular (NNV) AMD eyes when compared to neovascular (NV) AMD fellow eyes.

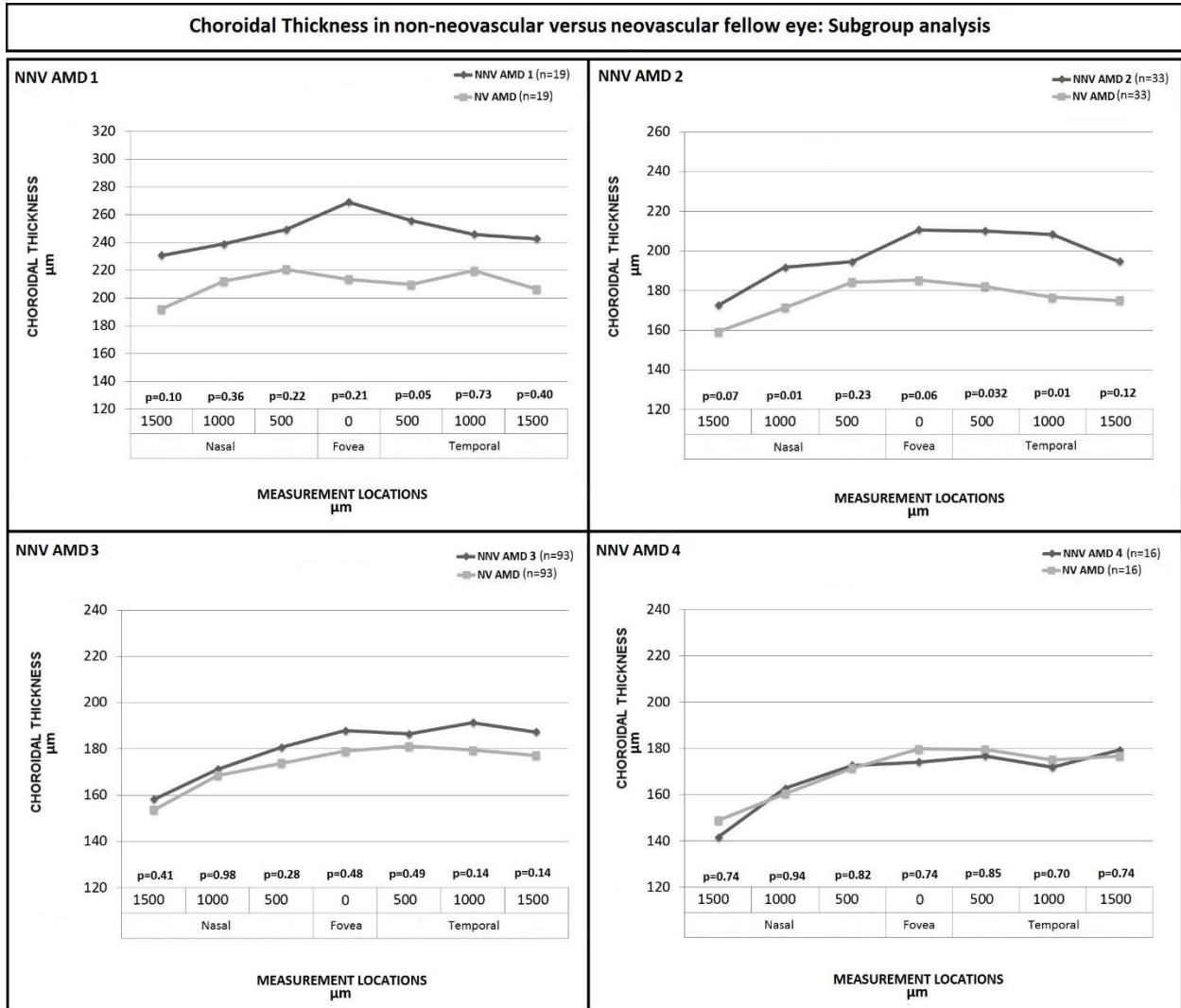
While CT was lower in the NNV AMD eyes at all positions tested, the difference was not statistically significant nasal to the macula. The choroid is thinnest within the nasal macular region in the normal population and it may be more difficult to detect significant CT changes in this area due to a statistical “floor” effect.

Another possible explanation is that in AMD choroidal thinning may not be uniform and may vary between distinct choroidal areas within the macular region. Choroidal circulation is an end-arterial vascular bed with segmental blood flow and watershed zones and therefore, the reaction of the choroid to different pathological mechanisms, including ischemia, may differ according to the location relative to the watershed zones.²⁷

When CT in the four subgroups of NNV AMD was compared using a linear regression model adjusted for age, significant differences were identified: a thicker choroid was noted at earlier stages of NNV AMD (Groups 1 and 2). These results, similar to those presented by Lu et al. and Lee et al., may suggest that the progression of NNV AMD may be associated with choroidal thinning.^{78,79}

This was further corroborated in our study. We performed a comparative analysis between CT of NNV AMD eyes versus the fellow NV AMD eyes for each stage of dry AMD and showed greater CT differences at earlier stages of NNV AMD (Groups 1 and 2), as illustrated in figure 34. The results of our study are the first to show a progressive reduction in CT difference directly correlated with the stage of NNV AMD using the fellow neovascular eye as the control group.

Figure 34



p-value: Wilcoxon Test

Our results differ from those presented by Yiu et al. and Jonas et al., who did not find significant differences between eyes with advanced and intermediate AMD versus a group of healthy controls without AMD, after age adjustment.^{22,23} The reasons of such discrepancies are uncertain, but probably driven by differences in study design and the lack of a fellow-eye analysis, which may have produced higher inter-group variability.

The majority of our patients with NV AMD received intravitreal anti-VEGF treatment, which may cause significant choroidal thinning. Ting et al., in a prospective

fellow-eye study with a follow up of 12 months, demonstrated choroidal thinning after monthly intravitreal injections of anti-VEGF in NV AMD.⁸⁰ However, CT has been shown to decrease significantly during the first three months of anti-VEGF therapy, and then stabilize. In our study CT was measured at a mean of 4.9 ± 3.9 months after the last anti-VEGF injections and this may have limited the confounding effect of anti-VEGF therapy.

Systemic absorption of intravitreal anti-VEGF drugs into the bloodstream may occur, and may have influenced CT in the untreated fellow eye in our study.

However, Mazaraki et al. showed no significant CT differences in fellow eyes of pretreated NV AMD eyes after intravitreal Anti-VEGF therapy.⁸¹

In the present report, comparative CT analysis between treatment-naïve and anti-VEGF treated NV AMD eyes was not performed due to the small number of untreated eyes.

Although the effect of Anti-VEGF therapy on CT remains an open issue as longitudinal observational studies of untreated active NV AMD are unlikely to be pursued, Rishi et al. retrospectively described thinner CT in treatment-naïve NV AMD eyes if compared with healthy controls.³² Such results suggest that choroidal thinning in NV AMD may occur independently of Anti-VEGF therapy. Moreover, as reported by McDonnell et al, our study estimated a CT decrease rate at each year of age that was almost identical in NNV AMD ($3.93\mu\text{m}$) and NV AMD fellow eyes ($3.31\ \mu\text{m}$), suggesting that anti-VEGF therapy did not accelerate CT decline.⁸²

This study has some important limitations, including its retrospective design and the absence of a control group without anti-VEGF treatment. Since anti-VEGF agents may alter CT, is it possible that our results may have been biased by this confounding factor. Moreover, although a fellow-eye design helps in reducing confounders, previous

reports showed significant differences in CT between both eyes of the same patient. For example, Ruiz-Medrano et al. reported significant differences in nasal CT between left and right eye of healthy subjects.⁷¹ Similarly, Chen et al. and Kang et al. described discrepancies in sub-foveal CT in normal populations.^{72,73}

However, even considering these limitations, the results of the present study are noteworthy as, to the best of our knowledge, the progressive reduction of CT across all stages of NNV AMD, described in our paper, was not previously reported in a fellow-eye comparison. These findings suggest a significant correlation between CT and AMD status, and remark the integral role of the choroid in the pathogenesis of AMD.

Future studies will likely rely on a new OCT technology called OCT angiography (OCT-A). OCT-A is a next-generation technology that differently to conventional OCT allows to quantify non-invasively choroidal blood flow in different choroidal layers (figure 35).⁸³

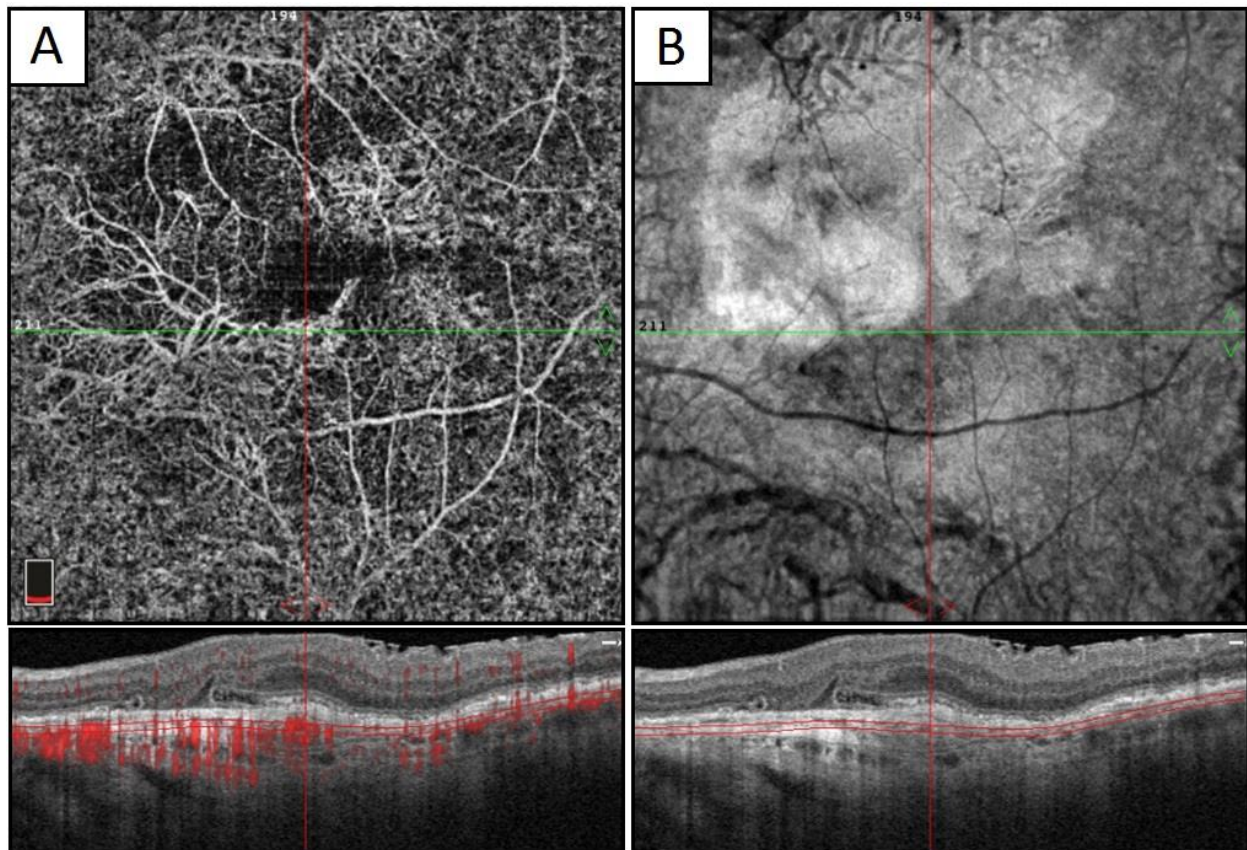
Recent investigations have focused on the composition of choriocapillaris and choroid in patients featuring early stages of non-neovascular AMD.⁸⁴

Abnormalities in the choriocapillaris or blood flow have been implicated as a potential risk factor in the pathogenesis of macular diseases, particularly for AMD, and OCT-A imaging will be a powerful diagnostic tool in choroidal assessment. Spaide found measureable choriocapillaris flow alterations associated with late AMD in the fellow eye, confirming that the choriocapillaris flow may be one factor in the development of late AMD.⁸⁴

Cicinelli et al. found a reduction that is numerically more significant in the choroidal thickness, in the vessel density at the choriocapillaris in non-neovascular AMD,

contributing to the body of evidence that the choriocapillaris flow may be one factor in the development of late AMD.⁸⁵

Figure 35:



Optical Coherence Tomography Angiography in age related macular degeneration.

A. OCT-A of a choroidal neovascular membrane. Segmentation at the level of the RPE-Bruch-Chriocapillaris complex. **B.** En-face imaging of the choroidal neovascular membrane.

In conclusion, our study described a significantly thicker choroid in the macula especially at the subfoveal and temporal positions in NNV AMD eyes when compared with NV AMD

fellow eyes. Furthermore, significant CT differences were shown between subgroups of NNV AMD eyes, with a thicker choroid noted at earlier stages of NNV AMD. Our results should be interpreted with caution. Further larger, longitudinal studies are necessary to reduce the risk of bias and to further elucidate the nature and extent of choroidal thinning in NV AMD and its relation to anti-VEGF therapies.

5 CONCLUSIONS

1. In non-neovascular AMD, our study described a significantly thicker macular choroid, if compared to neovascular AMD fellow eyes.
2. Significant choroidal thickness differences were shown between subgroups of non-neovascular AMD eyes, with a thicker choroid noted at earlier stages of non-neovascular AMD.

6. REFERENCES

1. Margolis R, Spaide RF. A pilot study of enhanced depth imaging optical coherence tomography of the choroid in normal eyes. *Am J Ophthalmol*. 2009;147:811-815.
2. Tan KA, Gupta P, Agarwal A, et al. State of science: choroidal thickness and systemic health. *Surv Ophthalmol* Published Online First: 12 Mar 2016. doi:10.1016/j.survophthal.2016.02.007
3. Chung SE, Kang SW, Lee JH, et al. Choroidal thickness in polypoidal choroidal vasculopathy and exudative age-related macular degeneration. *Ophthalmology* 2011;118:840–5.
4. Flores-Moreno I, Lugo F, Duker JS, et al. The relationship between axial length and choroidal thickness in eyes with high myopia. *Am J Ophthalmol* 2013;155:314–19.
5. Lee K, Lee J, Lee CS, et al. Topographical variation of macular choroidal thickness with myopia. *Acta Ophthalmol* 2015;93:e469–74.
6. Pang CE, Sarraf D, Freund KB. Extreme choroidal thinning in high myopia. *Retina* 2015;35:407–15.
7. Banitt M. The choroid in glaucoma. *Curr Opin Ophthalmol* 2013;24:125–9.
8. Yan H, Li J, Zhang J, et al. Retinal and choroidal thickness in patients with uveitis. *Ocul Immunol Inflamm* Published Online First: 29 Dec 2015. doi:10.1186/1471-2415-14-103
9. Melancia D, Vicente A, Cunha JP, et al. Diabetic choroidopathy: a review of the current literature. *Graefes Arch Clin Exp Ophthalmol* 2016;254:1453–61.
10. Warrow DJ, Hoang QV, Freund KB. Pachychoroid pigment epitheliopathy.

Retina 2013;33:1659–72.

11. Pang CE, Freund KB. Pachychoroid neovasculopathy. *Retina* 2015;35:1–9.
12. Wei WB, Xu L, Jonas JB, et al. Subfoveal choroidal thickness: the Beijing Eye Study. *Ophthalmology* 2013;120:175–80.
13. Friedman E. A hemodynamic model of the pathogenesis of age-related macular degeneration. *Am J Ophthalmol* 1997;124:677–82.
14. Grunwald JE, Hariprasad SM, DuPont J, et al. Foveolar choroidal blood flow in age-related macular degeneration. *Invest Ophthalmol Vis Sci* 1998;39:385–90.
15. Grunwald JE, Metelitsina TI, Dupont JC, et al. Reduced foveolar choroidal blood flow in eyes with increasing AMD severity. *Invest Ophthalmol Vis Sci* 2005;46:1033–8.
16. Xu W, Grunwald JE, Metelitsina TI, et al. Association of risk factors for choroidal neovascularization in age-related macular degeneration with decreased foveolar choroidal circulation. *Am J Ophthalmol* 2010;150:40–7.
17. Sigler EJ, Randolph JC. Comparison of macular choroidal thickness among patients older than age 65 with early atrophic age-related macular degeneration and normals. *Invest Ophthalmol Vis Sci* 2013;54:6307–13.
18. Lee JY, Lee DH, Lee JY, et al. Correlation between subfoveal choroidal thickness and the severity or progression of nonexudative age-related macular degeneration. *Invest Ophthalmol Vis Sci* 2013;54:7812–18.
19. Kim SW, Oh J, Kwon SS, et al. Comparison of choroidal thickness among patients with healthy eyes, early age-related maculopathy, neovascular age-related macular degeneration, central serous chorioretinopathy, and polypoidal choroidal vasculopathy. *Retina* 2011;31:1904–11.

20. Manjunath V, Goren J, Fujimoto JG, et al. Analysis of choroidal thickness in age-related macular degeneration using spectral-domain optical coherence tomography. *Am J Ophthalmol* 2011;152:663–8.
21. Wood A, Binns A, Margrain T, et al. Retinal and choroidal thickness in early age-related macular degeneration. *Am J Ophthalmol* 2011;152:1030–38.e2.
22. Jonas JB, Forster TM, Steinmetz P, et al. Choroidal thickness in age-related macular degeneration. *Retina* 2014;34:1149–55.
23. Yiu G, Chiu SJ, Petrou PA, et al. Relationship of central choroidal thickness with age-related macular degeneration status. *Am J Ophthalmol* 2015;159:617–26.
24. Parver LM, Heiduschka P, Julien S, et al. Choroidal blood flow as a heat dissipating mechanism in the macula. *Am J Ophthalmol*. 1980;89:641-6.
25. Alm A, Bill A. Ocular and optic nerve blood flow at normal and increased intraocular pressures in monkeys (*Macaca Iru*s): a study with radioactively labelled microspheres including flow determination in brain and some other tissues. *Exp Eye Res*. 1973;15:15-29.
26. Hayreh SS. In vivo choroidal circulation and its watershed zones. *Eye (Lond)* 1990;4:273–89.
27. Hayreh SS. Posterior Ciliary Artery Circulation in Health and Disease. The Weisenfeld Lecture. *Invest Ophthalmol Vis Sci* 2004;45:749–57.
28. Rhodes LA, Huisinigh C, Johnstone J, et al. Peripapillary choroidal thickness variation with age and race in normal eyes. *Invest Ophthalmol Vis Sci* 2015;56:1872–9.
29. Barteselli G, Chhablani J, El-Emam S, et al. Choroidal volume variations with age, axial length, and sex in healthy subjects: a three-dimensional analysis.

Ophthalmology 2012;119:2572–8.

30. Li XQ, Larsen M, Munch IC. Subfoveal choroidal thickness in relation to sex and axial length in 93 Danish university students. *Invest Ophthalmol Vis Sci* 2011;52:8438–41.
31. Ahn SJ, Woo SJ, Park KH. Retinal and choroidal changes with severe hypertension and their association with visual outcome. *Invest Ophthalmol Vis Sci* 2014;55:7775–85.
32. Rishi P, Rishi E, Mathur G, et al. Ocular perfusion pressure and choroidal thickness in eyes with polypoidal choroidal vasculopathy, wet-age-related macular degeneration, and normals. *Eye (Lond)* 2013;27:1038–43.
33. Brown JS, Flitcroft DI, Ying GS, et al. In vivo human choroidal thickness measurements: evidence for diurnal fluctuations. *Invest Ophthalmol Vis Sci* 2009;50:5–12.
34. Usui S, Ikuno Y, Akiba M, et al. Circadian changes in subfoveal choroidal thickness and the relationship with circulatory factors in healthy subjects. *Invest Ophthalmol Vis Sci* 2012;53:2300–7.
35. Sizmaz S, Küçükerdönmez C, Pinarci EY, et al. The effect of smoking on choroidal thickness measured by optical coherence tomography. *Br J Ophthalmol* 2013;97:601–4.
36. He M, Han X, Wu H, et al. Choroidal thickness changes in obstructive sleep apnea syndrome: a systematic review and meta-analysis. *Sleep Breath* 2016;20:369–78.
37. Yilmaz I, Ozkaya A, Kocamaz M. Correlation of choroidal thickness and body mass index. *Retina* 2015;35:2085–90.

38. Kim DY, Silverman RH, Chan RV, et al. Measurement of choroidal perfusion and thickness following systemic sildenafil (Viagra®). *Acta Ophthalmol* 2013;91:183–8.
39. Nickla DL, Wallman J. The multifunctional choroid. *Prog Retin Eye Res*. 2010;29:144-68.
40. Hayreh SS. In vivo choroidal circulation and its watershed zones. *Eye (Lond)*. 1990;4:273-89.
41. Wong WL, Su X, Li X, et al. Global prevalence of age-related macular degeneration and disease burden projection for 2020 and 2040: a systematic review and meta-analysis. *Lancet Glob Health*. 2014;2(2):e106-16.
42. Ferris FL 3rd, Wilkinson CP, Bird A, et al. Beckman Initiative for Macular Research Classification Committee. Clinical classification of age-related macular degeneration. *Ophthalmology*. 2013;120:844-51.
43. Chew EY, Clemons TE, Agrón E, et al. Ten-year follow-up of age-related macular degeneration in the age-related eye disease study: AREDS report no. 36. *JAMA Ophthalmol*. 2014;132:272-7.
44. Shim SH, Kim SG, Bae JH, Yu HG, Song SJ. Risk Factors for Progression of Early Age-Related Macular Degeneration in Koreans. *Ophthalmic Epidemiol*. 2016;23:80-7.
45. Friedman E. The role of the atherosclerotic process in the pathogenesis of age-related macular degeneration. *Am J Ophthalmol* 2000;130:658–63.
46. Friedman E. A hemodynamic model of the pathogenesis of age-related macular degeneration. *Am J Ophthalmol* 1997;124:677–82.

47. Friedman E, Smith T, Kuwabara T. Senile choroidal vascular patterns and drusen. *Arch Ophthalmol* 1963;69:220–30.
48. Malek G, Li CM, Guidry C, et al. Apolipoprotein B in cholesterol-containing drusen and basal deposits of human eyes with age-related maculopathy. *Am J Pathol* 2003;162:413–25.
49. Friedman E, Ivry M, Ebert E, et al. Increased scleral rigidity and age-related macular degeneration. *Ophthalmology* 1989;96:104–8.
50. Friedman E, Krupsky S, Lane A, et al. Ocular blood flow velocity in age-related macular degeneration. *Ophthalmology* 1995;102:640–6.
51. Broekhuysen RN. The lipid composition of aging sclera and cornea. *Ophthalmologica* 1975;171:82–5.
52. Friedman E. Update of the vascular model of AMD. *Br J Ophthalmol*. 2004; 88: 61–163.
53. Prunte C, Niesel P. Quantification of choroidal blood-flow parameters using indocyanine green video-fluorescence angiography and statistical picture analysis. *Graefes Arch Clin Exp Ophthalmol*. 1988;226:55-8.
54. Ciulla TA, Harris A, Kagemann L, et al. Choroidal perfusion perturbations in non-neovascular age related macular degeneration. *Br J Ophthalmol*. 2002;86:209-13.
55. Grunwald JE, Metelitsina TI, Dupont JC, Ying GS, Maguire MG. Reduced foveolar choroidal blood flow in eyes with increasing AMD severity. *Invest Ophthalmol Vis Sci*. 2005;46:1033-8.
56. Xu W, Grunwald JE, Metelitsina TI, et al. Association of risk factors for choroidal neovascularization in age-related macular degeneration with decreased foveolar choroidal circulation. *Am J Ophthalmol*. 2010;150:40-47.

57. Mori F, Konno S, Hikichi T, Yamaguchi Y, Ishiko S, Yoshida A. Pulsatile ocular blood flow study: decreases in exudative age related macular degeneration. *Br J Ophthalmol.* 2001;85:531-3.
58. Schmetterer L, Wolzt M. Laser interferometric investigations of pulsatile choroidal blood flow: review and new results on the validity of the technique. *J Biomed Opt.* 1998;3:246-52.
59. Brown JS, Flitcroft, ID, Ying GS, et al. In Vivo Human Choroidal Thickness Measurements: Evidence for Diurnal Fluctuations. *Invest Ophthalmol Vis Sci.* 2009;50:5–12.
60. Wakatsuki Y, Shinojima A, Kawamura A, Yuzawa M1. Correlation of Aging and Segmental Choroidal Thickness Measurement using Swept Source Optical Coherence Tomography in Healthy Eyes. *PLoS One.* 2015 Dec 3;10:e0144156.
61. Grunwald JE, Metelitsina TI, Dupont JC, Ying GS, Maguire MG. Reduced foveolar choroidal blood flow in eyes with increasing AMD severity. *Invest Ophthalmol Vis Sci.* 2005;46:1033-8.
62. Whitmore SS, Sohn EH, Chirco KR, et al. Complement activation and choriocapillaris loss in early AMD: implications for pathophysiology and therapy. *Prog Retin Eye Res.* 2015;45:1-29.
63. Nunes RP, Rosa PR, Giani A, et al. Choroidal Thickness in Eyes With Central Geographic Atrophy Secondary to Stargardt Disease and Age-Related Macular Degeneration. *Ophthalmic Surg Lasers Imaging Retina.* 2015;46:814-22.
64. Mrejen S, Spaide RF. Optical coherence tomography: imaging of the choroid and beyond. *Surv Ophthalmol.* 2013 Sep-Oct;58:387-429.

65. Oguz I, Abramoff MD, Zhang L, Lee K, Zhang EZ, Sonka M. 4D Graph-Based Segmentation for Reproducible and Sensitive Choroid Quantification From Longitudinal OCT Scans. *Invest Ophthalmol Vis Sci.* 2016;57:OCT621-OCT630.
66. Shi F, Tian B, Zhu W, et al. Automated choroid segmentation in three-dimensional 1- μ m wide-view OCT images with gradient and regional costs. *J Biomed Opt.* 2016;1;21:126017.
67. Mazzaferri J, Beaton L, Hounye G, Sayah DN, Costantino S. Open-source algorithm for automatic choroid segmentation of OCT volume reconstructions. *Sci Rep.* 2017;9;7:42112.
68. Tan CS, Cheong KX. Macular choroidal thicknesses in healthy adults--relationship with ocular and demographic factors. *Invest Ophthalmol Vis Sci.* 2014; 55:(6452-8.
69. Mansouri K, Medeiros FA, Marchase N, Tatham AJ, Auerbach D, Weinreb RN. Assessment of choroidal thickness and volume during the water drinking test by swept-source optical coherence tomography. *Ophthalmology.* 2013;120:2508-16.
70. Ikuno Y, Kawaguchi K, Nouchi T, Yasuno Y. Choroidal thickness in healthy Japanese subjects. *Invest Ophthalmol Vis Sci.* 2010;51:2173-6.
71. Ruiz-Medrano J1, Flores-Moreno I, Peña-García P, Montero JA, Duker JS, Ruiz-Moreno JM. Asymmetry in macular choroidal thickness profile between both eyes in a healthy population measured by swept-source optical coherence tomography. *Retina.* 2015 Oct;35:2067-73.
72. Chen FK, Yeoh J, Rahman W, Patel PJ, Tufail A, Da Cruz L. Topographic variation and interocular symmetry of macular choroidal thickness using enhanced depth

- imaging optical coherence tomography. *Invest Ophthalmol Vis Sci.* 2012;53:975-85.
73. Kang HM, Kim SJ, Koh HJ, Lee CS, Lee SC. Discrepancy in Subfoveal Choroidal Thickness in Healthy Adults with Isometropia. *Ophthalmology.* 2015;122:2363-4.
74. Esmaeelpour M, Kajic V, Zabihian B, et al. Choroidal Haller's and Sattler's layer thickness measurement using 3-dimensional 1060-nm optical coherence tomography. *PLoS One.* 2014 Jun 9;9:e99690.
75. Ramrattan RS1, van der Schaft TL, Mooy CM, de Bruijn WC, Mulder PG, de Jong PT. Morphometric analysis of Bruch's membrane, the choriocapillaris, and the choroid in aging. *Invest Ophthalmol Vis Sci.* 1994;35:2857-64.
76. Duan XR, Liang YB, Friedman DS, et al. Normal macular thickness measurements using optical coherence tomography in healthy eyes of adult Chinese persons: the Handan Eye Study. *Ophthalmology.* 2010;117:1585-94
77. Kinoshita T, Mitamura Y, Shinomiya K, et al. Diurnal variations in luminal and stromal areas of choroid in normal eyes. *Br J Ophthalmol.* 2016 Jun 13. pii: bjophthalmol-2016-308594.
78. Lu L, Xu S, He F, et al. Assessment of Choroidal Microstructure and Subfoveal Thickness Change in Eyes With Different Stages of Age-Related Macular Degeneration. *Medicine (Baltimore).* 2016;95:e2967.
79. Lee JY, Lee DH, Lee JY, Yoon YH. Correlation between subfoveal choroidal thickness and the severity or progression of nonexudative age-related macular degeneration. *Invest Ophthalmol Vis Sci.* 2013;54:7812-8.

80. Ting DS, Ng WY, Ng SR, et al. Choroidal Thickness Changes in Age-Related Macular Degeneration and Polypoidal Choroidal Vasculopathy: A 12-Month Prospective Study. *Am J Ophthalmol.* 2016 ;164:128-36.e1.
81. Mazaraki K, Fasnacht-Riederle H, Blum R, Becker M, Michels S. Change in choroidal thickness after intravitreal aflibercept in pretreated and treatment-naive eyes for neovascular age-related macular degeneration. *Br J Ophthalmol.* 2015;99:1341-4.
82. McDonnell EC, Heussen FM, Ruiz-Garcia H, et al. Effect of anti-VEGF treatment on choroidal thickness over time in patients with neovascular age-related macular degeneration. *Eur J Ophthalmol.* 2014;24:897-903.
83. Cole ED, Ferrara D, Novais EA, Louzada RN, Waheed NK. Clinical trial endpoints for optical coherence tomography angiography in neovascular age-related macular degeneration. *Retina.* 2016 Dec;36 Suppl 1:S83-S92.
84. Richard F. Spaide. Choriocapillaris Flow Features Follow a Power Law Distribution: Implications for Characterization and Mechanisms of Disease Progression. *Am J Ophthalmol.* 2016;170:58-67.
85. Cicinelli MV, Rabiolo A, Marchese A, et al. Choroid morphometric analysis in non-neovascular age-related macular degeneration by means of optical coherence tomography angiography. *Br J Ophthalmol* 2017 Jan 5 [Epub ahead of print].